




# THE SCINTIRAD PROJECT



DEVELOPMENT OF NUCLEAR DETECTORS  
AND RADIOPHARMACEUTICALS  
FOR IMAGING AND THERAPY IN ONCOLOGY

# THE SCINTIRAD PROJECT

## DEVELOPMENT OF NUCLEAR DETECTORS AND RADIOPHARMACEUTICALS FOR IMAGING AND THERAPY IN ONCOLOGY

G. Moschini, P. Boccaccio, M. Laveder, P. Rossi, N. Uzunov, M. Bello  
*Department of Physics of the University of Padua and INFN*

D. Bollini, F.L. Navarria, G. Baldazzi, A. Perrotta, M. Zuffa  
*Department of Physics of the University of Bologna and INFN*

F. de Notaristefani, V. Orsolini Cencelli  
*Department of Electronic Engineering of the University of Rome-3 and INFN*

R. Pani, R. Pellegrini  
*Department of Experimental Medicine and Pathology, University of Rome-1 and INFN*

M. Mattioli, M.N. Cinti, P. Bennati, M. Betti, V. Casali  
*Department of Physics of the University of Rome-1 and INFN*

R. Scafè  
*ENEA-Casaccia and INFN*

C. Tanzarella, A. Antoccia  
*Department of Biology of the University of Rome-3 and INFN*

U. Mazzi, L. Melendez-Alafort, A. Nadali, E. Zangoni  
*Department of Pharmaceutical Sciences of the University of Padua*

G.P. Giron, M.C. Giron, C. Ori,  
*Department of Pharmacology and Anesthesiology of the University of Padua*

D. Bernardini, A. Zotti, G. Gerardi, H. Poser  
*Department of Clinical Veterinary Sciences of the University of Padua*

A. Rosato, A. Banzato  
*Department of Oncology and Surgical Sciences of the University of Padua*

G. Sotti, D. Casara  
*IOV (Istituto Oncologico Veneto). Unit of Radiotherapy and Nuclear Medicine*

### Abstract

Scintirad is an interdisciplinary research program that studies novel translational radiopharmaceuticals for cancer diagnosis and therapy. Scintirad employs methods of the Nuclear Medicine applied to small animals and develops new instrumentation for high resolution imaging. The first part of this report describes research programs, results and future plans, while the second part, entitled "who we are", offers an overview of the role of involved teams and facilities.



## SUMMARY

<b>INTRODUCTION</b>	<b>1</b>
---------------------	----------

### **I PART: RESEARCH PROGRAMS, RESULTS AND FUTURE PLANS**

#### **RESEARCH PROGRAMS**

-INTRODUCTION	5
-NEW DETECTORS FOR IMAGING	6
-RADIOPHARMACEUTICALS	7
-THERAPEUTIC APPROACHES	7
-RADIOBIOLOGY	8

#### **RESULTS AND FUTURE PLANS**

-AN ENHANCED EXPERIMENTAL SET-UP BASED ON H8500 PSPMT'S	11
-STUDIES ON THE LABR3:CE SCINTILLATOR	18
-MEASURING THE IMAGED-OBJECT DISTANCE WITH A STATIONARY HIGH-SPATIAL-RESOLUTION SCINTILLATION CAMERA (A PATENT)	31
-MEDICAL AND PHARMACOLOGICAL ACHIEVEMENTS OF THERAPEUTIC IMPACT	38

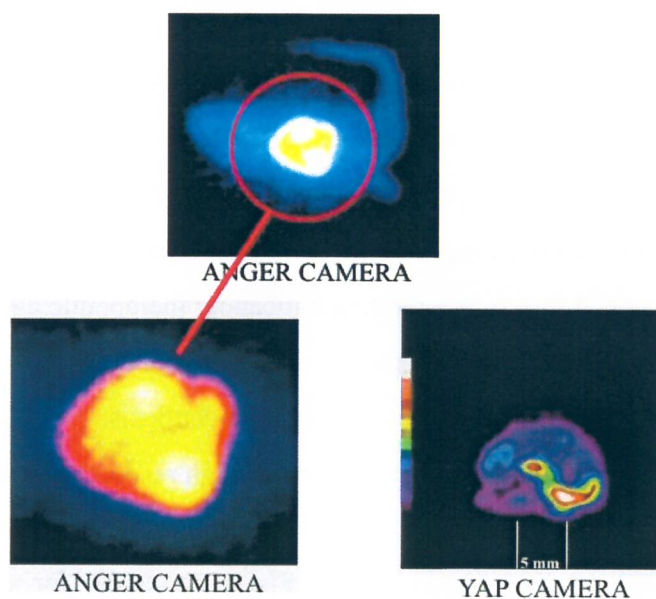
### **II PART: WHO WE ARE**

THE LRRS (LNL – INFN) LABORATORY (LEGNARO, PADOVA)	49
THE VETERINARY CLINICS IN AGRIPOLIS (LEGNARO, PADOVA)	55
THE BOLOGNA UNIVERSITY AND INFN TEAM	59
THE ROME I UNIVERSITY AND INFN TEAM	61
THE LMIC (INFN - ROMA III) LABORATORY	63
THE NUCLEAR MEDICINE SERVICE (IOV, PADOVA)	67

<b>PUBBLICATIONS</b>	<b>73</b>
----------------------	-----------

## INTRODUCTION

Nuclear medicine is a branch of medicine that involves oral or intravenous administration of radioactive materials for use in diagnostics and therapy. Most of radiopharmaceuticals available (95%) are used in diagnostics. These allow the determination of organ's function, shape, position and other clinical information from an image of the distribution of the radio-pharmaceuticals administered to the body. The radiopharmaceutical localizes in organs and tissues according to its biological or physiological properties. The gamma-ray radiation from the radiopharmaceutical is externally detected by a scintillation detector (often a sodium iodide crystal) that converts the absorbed gamma-ray energy into visible light. Photomultipliers convert the light to electronic signals, which are eventually processed to obtain the radiopharmaceuticals' position.



*Images of a BALB/c mouse obtained with a conventional Nuclear Medicine Anger Camera and a new design YAP camera. The mouse has been inoculated with  $^{99m}\text{Tc}$  MDP, a bone seeking agent.*

Scintillation detectors sensible to the gamma-ray position are widely exploited in the nuclear medicine. They are known as “Anger cameras” or “gamma cameras” and are capable to produce either planar images (Scintigraphy, or SPET – Single Photon Emission Tomography) or three-dimensional information (SPECT: Single Photon Emission Computed Tomography).



New concept gamma-ray cameras based on highly segmented detectors are recently introduced to achieve higher spatial resolution (details of 1 mm and even less) of the imaged organs. To this purpose new kinds of scintillators having suitable scintillation properties (efficiency, density, luminosity, transparency, etc.) and appropriate mechanical properties (in order to be shaped in small cells (pillars)) are today developed. Position-sensitive detectors equipped with segmented scintillators such as YAP (Yttrium Aluminum Perovskite  $\text{YAlO}_3$ , doped with Cerium) or  $\text{LaBr}_3$  (also exploited in this project) are the most promising imaging instruments.

Isotopes that are both gamma- and beta- emitters, capable to delay the functions of the cells or to destroy them, may be effectively used also in the therapy, especially in the tumor treatment. A significant number of research projects are devoted to the exploitation of their joint diagnostic and therapeutic capabilities.

SCINTIRAD is a project focused on interdisciplinary research aiming to meliorate the existing routines and to develop new and effective methods for cancer diagnosis and therapy. To realise this idea the following activities are conducted:

- testing novel translational radiopharmaceuticals for cancer diagnosis and therapy;
- clarifying the mechanisms of radiobiological damage induced by some beta-ray emitters and studying the possibility to use them as anticancer therapeutic agents;
- employing Nuclear Medicine methods to small animals in order to study the biodistribution of the new synthesized radiopharmaceuticals;
- developing new methods and instrumentation for high resolution gamma-ray imaging.

The project SCINTIRAD has been mainly funded by the National Institute for Nuclear Physics INFN (Istituto Nazionale di Fisica Nucleare) for several years and it is carried out by a national collaboration involving teams located in Rome, Bologna, Padua and LNL (Legnaro National Laboratories). Other sources have funded sectors not involved in detectors development.

SCINTIRAD has put together a rich expertise for developing different parts, including innovative detectors (Rome), a scintigraphic setup (Bologna and Padua), the radiopharmaceuticals (Padua), a medical and veterinary environment allowing for in-vivo tests (Agripolis, Padua) and the medical rationale (Medical School, Padua).

The LNL Laboratories, for their experimental excellence, technical support and proximity to the medical and veterinary teams, have become the hub where devices have been assembled and experiments carried out. In particular, SCINTIRAD employs the “Laboratory of Radioisotope and Radiopharmaceutical Studies” (LRRS), which has been founded in collaboration with the Department of Pharmacology and Anesthesiology of the University of Padua, and houses advanced nuclear medicine instrumentation and detectors to image the bio-distribution of radio-pharmaceuticals. The LRRS is fully authorized to a Nuclear Medicine practice and accordingly radio-protected. The proximity to the Agricultural and Veterinary Faculties of the University of Padua (Agripolis) promotes cooperation on subjects of common interest and exchange of instrumentation and methodology, including the in-vivo experimentation on animals.

The paper is divided in two parts:

- Research programs, results and future plans;
- Who we are, i.e. description of the teams involved in Scintirad and their contribution to the experiment.



## I PART

### RESEARCH PROGRAMS, RESULTS AND FUTURE PLANS

#### RESEARCH PROGRAMS

##### INTRODUCTION

We study the effectiveness of some radio-pharmaceuticals to attack cancer and more generally the radiation damage they induce, by imaging their bio-distribution in small animals.

A radiation emitting drug may also have a therapeutic impact, if able to selectively target tumor cells. To this purpose, the radio-nuclide should emit beta or alpha radiations, beside the gammas used for imaging. We have employed the  $^{188}\text{Re}$ , featuring two main emissions: a beta component (85%) well suited for radiotherapy and a gamma component (15%) for scintigraphy. One can obtain the Rhenium-188 by from a commercial generator  $^{188}\text{W}/^{188}\text{Re}$  that has a few months lifetime. The  $^{188}\text{Re}$ -labeling of bio-molecules may often follow the path already studied for Technetium that has similar chemical properties, and produces a comparable bio-distribution. Moreover, one may exploit the same detector that is used for Tc, since Re emits gammas of similar energy. We currently employ  $^{99}\text{Tc}$  radio-pharmaceuticals during the tuning of the diagnostic, and  $^{188}\text{Re}$  radio-pharmaceutical in radiotherapy.

In particular, we study, employing a pre-clinic experimental model, the conjugate  $^{188}\text{Re}$ -Hyaluronic acid ( $^{188}\text{Re}$ -HA) and its therapeutic effectiveness on cancer that is located exclusively or preferentially in liver. This approach relies upon several results we have already obtained, pointing out the HA or HA conjugates do nearly exclusively concentrate in liver after intravenous inoculation. This may suggest a true local-regional treatment, to be carried out with no risky and costly surgery, and moreover with high therapeutic effectiveness and no side effects.

The results show a dose-answer effect as for the tumor growing suppression, suggesting that this approach may be employed in vivo.

To inspect structures in organs of small animals inoculated with gamma emitting radiopharmaceuticals, we have developed innovative gamma detectors with sub-millimeter spatial resolution. We want to obtain morphological and especially functional information on organs and systems.

We detail the main research lines in the following

## NEW DETECTORS FOR IMAGING

We have employed a new design small gamma camera, equipped with a parallel hole collimator, and a highly segmented yttrium-aluminate perovskite (YAP) scintillator coupled to a position-sensitive photomultiplier (Hamamatsu R2486) that provides high resolution images (about 1 mm) on a field of 4x4 cm. This setup is used to assess in vivo biodistribution in mice, of  $^{99}\text{Tc}$ -labelled new prototype derivative bio-conjugates, consisting of cytotoxic drugs linked to biocompatible polysaccharides. The images shown at page 3 have been obtained from a  $^{99\text{m}}\text{Tc}$  line source and a BALB/c mouse, which has been inoculated with  $^{99\text{m}}\text{Tc}$  MDP, a bone seeking agent. These images show the importance of a small field YAP camera in radiopharmaceutical research.

To enhance the YAP camera information, we are also developing SPECT (Single Photon Emission Computerized Tomography) instrumentation, capable of a tri-dimensional imaging and a bigger field of view. This latter,  $10 \times 5 \text{ cm}^2$ , allows the inspection of slightly larger animals, like rats or other rodents, mostly used in pre-clinic tests. Their size is also compatible with micro-surgery, like heart and kidney transplants, prostate manipulation, intra-portal inoculation, cathetering of femoral artery, etc., offering further important scintigraphic applications.

The new detector features high resolution position-sensitive photomultipliers (Hamamatsu PSPMT H 9500), a new design 256 channel front-end and acquisition electronics, and a high efficiency and energy resolution LaBr3 detector ( $50 \times 50 \text{ mm}^2$ ). The collimator is now substantially thicker (40 mm) and capable to stop also the 200 keV gamma emission of Re-188. Finally a micrometric stage allows a circular positioning of the detector around the test animal, in order to have different views of the same organ, avoid superposition of two organs and improve the general signal to noise ratio.



## RADIOPHARMACEUTICALS

Technetium-99 and Rhenium-188 are two radio nuclides with similar chemical properties that allow for both imaging and therapy. The Department of Pharmaceutical Sciences of the University of Padova has been involved in the synthesis and characterization of Tc and Re complexes for many years. A pharmacology group of this Department, taking advantage of several labelling experiments at the LLRS-LNL Laboratory, has considered and developed pharmaceuticals ready to be investigated for their capability of imaging and treating cancer.

Hyaluronic acid has been directly labelled with Tc-99m and the bio-distribution in vivo has been investigated with different administration methods. When injected in the blood pool,  $^{99m}\text{Tc}$ -Hyal has been found 80% in the liver after 10 minutes. In all the other cases, the radiotracer almost totally remains in the site of injection. A similar result was obtained with a  $^{188}\text{Re}$  labelling.

According to the BFCA strategy, other bioactive molecules have been labelled. In particular the PN2S coordinating set has been studied from the chemical point of view and it was used as BFCA for the conjugation to Mabs, peptides, or biotine.

The use of a linker such as PEG allowed for modification of the delivery properties of the whole labeled bio-molecule and for obtaining suitable radiopharmaceuticals for cancer imaging (Tc-99m) and radiotherapy (Re-188)

## THERAPEUTIC APPROACHES

Radiopharmaceuticals under development are based on three different approaches represented by (a) a natural polymer, Hyaluronic Acid (HA), (b) a mAb directed to PSMA, and (c) a Locked Nucleic Acid (LNA) capable of specific binding to survivin mRNA. These targeting molecules will be labelled with  $^{99m}\text{Tc}$  and  $^{188}\text{Re}$  for both imaging and therapy of tumors arising in liver, prostate and at multiple sites, respectively. The choice of such approaches is based on several considerations: our previous observations showed that  $^{99m}\text{Tc}$ -radiolabelled HA undergoes a selective hepatic uptake following i.v. administration. Therefore, it is conceivable that concentrating a  $^{188}\text{Re}$ -HA bioconjugate in the liver may lead to a very efficient loco-regional therapy obtainable without surgical interventions and

with reduced side-effects. In the framework of an existing collaboration, we are testing a mAb recognizing PSMA, a tumor-specific antigen of human prostate tumors. Cytofluorimetric studies have verified that biotinylation process did not alter binding capacity of the mAb, nor its interaction with avidin. These elements support testing a three-step pretargeting strategy involving i) inoculation of biotinylated mAb to bind target cells; ii) administration of avidin capable of interacting with the tumor-bound mAb and chasing unbound material; iii) injection of  $^{188}\text{Re}$ -biotin that will interact with the mAb-avidin complex on tumor cells to exert diagnostic and therapeutic effects. Finally, the third approach exploits the unique properties of the LNA technology together with the peculiar expression of survivin in cancer cells to develop a novel tumour targeting strategy. Indeed, survivin exhibits differential expression in nearly all human cancers while it is not expressed in most normal tissues, and this makes it a potentially attractive target for cancer therapeutics. To this end, we plan to develop survivin-specific LNA, small water-soluble synthetic antisense oligomers with exceptional biostability and enhanced hybridization performance towards complementary RNA, and to use them as carriers of diagnostic and therapeutic radio nuclides against survivin-expressing tumors.

## RADIOBIOLOGY

A critical point of antitumor radiopharmaceutics is represented by radiosensitivity of neoplastic cells and healthy tissues and by biological phenomena induced by irradiation. Indeed, scanty data are available in the literature on the *in vitro* and *in vivo* radioresponse of both normal and tumour cells after treatment with radiopharmaceutics characterized by beta-emission. To gain this piece of results it is particularly relevant considering that the radiosensitivity *in vitro* can predict the outcome of irradiation *in vivo*. To assess these points, studies are underway on culture cells and tumors and healthy tissue samples obtained from mice undergoing treatment with  $^{188}\text{Re}$ -labelled radiopharmaceutics. The capability of radiation to affect tumour cells *in vitro* will be evaluated with the MTT assay, which measures mitochondrial metabolism in the entire cell culture and is a recognized test for cytotoxicity and inhibition of cell proliferation. As an additional tool to monitor the radiosensitivity of treated cancer cells, the micronucleus test will be carried out. Micronuclei are small nuclei which arise as result of clastogenic damage, leading to a loss of chromosome



fragments at anaphase; this test is held as a valid measure of genotoxic damage. Finally, radio-induced apoptosis will be evaluated by means of three different approaches, that is scoring of apoptotic bodies, cells positive to the staining either to activated caspase-3 or TUNEL. In this latter test, the terminal deoxynucleotidyl transferase binds to 3'-OH ends of DNA fragments generated in response to apoptotic signals and catalyses the addition of biotin-FITC-labeled deoxynucleotides. To analyze irradiation-induced effects *in vivo*, radiobiological endpoints and apoptosis induction will be studied in tumours and in healthy tissues derived from animals treated with <sup>188</sup>Re-conjugated HA, biotin or LNA. In particular, immunohistochemistry techniques on paraffin-embedded tissue sections will allow to determine induction of those genes involved in the response to DNA damage and apoptosis, using monoclonal antibodies against p53, CDKN1A and bax. Apoptosis induction will be assessed by means of the TUNEL assay which is a suitable and reliable method to detect DNA fragmentation also in paraffin-embedded sections. Finally, molecular biology approaches based on quantitative Real Time RT-PCR conducted on mRNA extracted from frozen mouse tissue samples will allow the quantitation of bax, p53 and CDKN1A transcripts in order to determine the fold-induction of gene expression with respect to the basal level.

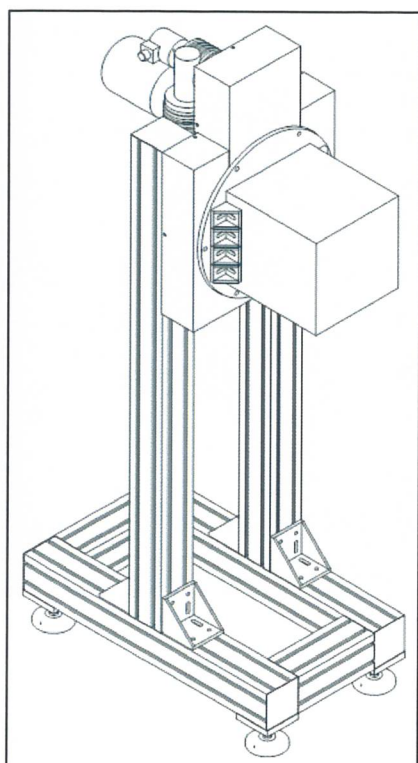
## RESULTS

This part is divided in a few sections highlighting some major achievements of SCINTIRAD: 1) An enhanced experimental set-up based on H8500 PSPMT's; 2) Studies on the LaBr<sub>3</sub>:Ce scintillator; 3) A method for measuring the object-to-detector distance with stationary high-spatial resolution cameras (Patent No RM 2006 A 000216, UIBM Roma; 4) Medical and Pharmacological achievements of therapeutic impact..

### 1) A NEW ENHANCED EXPERIMENTAL SET-UP BASED ON H8500 PSPMT's

#### I. Introduction

A new experimental set-up, recently developed, makes use of two position-sensitive photomultiplier tubes (PSPMT) Hamamatsu H8500 (Figure 1). The two PSPMT – plugged into



a separate boards – are coupled to a LaBr<sub>3</sub>:Ce scintillator slab and a parallel hole lead collimator (Figure 2), and housed inside a lead shield. The detectors are positioned at a relative angle of 90° and can inspect a mouse placed inside a triangular-shaped shielding (see Figure 3 and 4). All the detection system, constituted from the two H8500 PSPMT each one with its LaBr<sub>3</sub>:Ce scintillator slab and parallel hole collimator, will be mounted on a motorized rotating stage (Figure 1) to perform a tomographic reconstruction of the tracer inside the mouse under examination.

A brief explanation of the components follows.

Figure 1. *The rotating stage. The box in front of it represents the external housing of the detection system.*

## II. The H8500 flat panel

The Hamamatsu H8500 Flat Panel PSPMT is the most recent array photomultiplier tube, designed for small scintillation cameras. It is based on metal channel dynode technology and its external dimensions are  $52 \times 52 \times 14.4 \text{ mm}^3$  for an active area of  $49 \times 49 \text{ mm}^2$ . The anodic plane consists of a  $8 \times 8$  anode matrix, each pixel having a  $6.0 \times 6.0 \text{ mm}^2$  area, with reduced dead space. The photocathode is of the bi-alkali type, and the 12-stage multiplier furnishes a typical gain of  $10^6$  at  $-1100\text{V}$  anode voltage. The H8500 anode uniformity has been evaluated with a W-Lamp (Uniform DC Light), and turned to be quite acceptable (roughly 1:2). The photocathode sensitivity is in the range  $300\div 650\text{nm}$ , the typical dark current is  $32 \text{ nA}$ , and the transit time of the electrons is  $6\text{ns}$ .

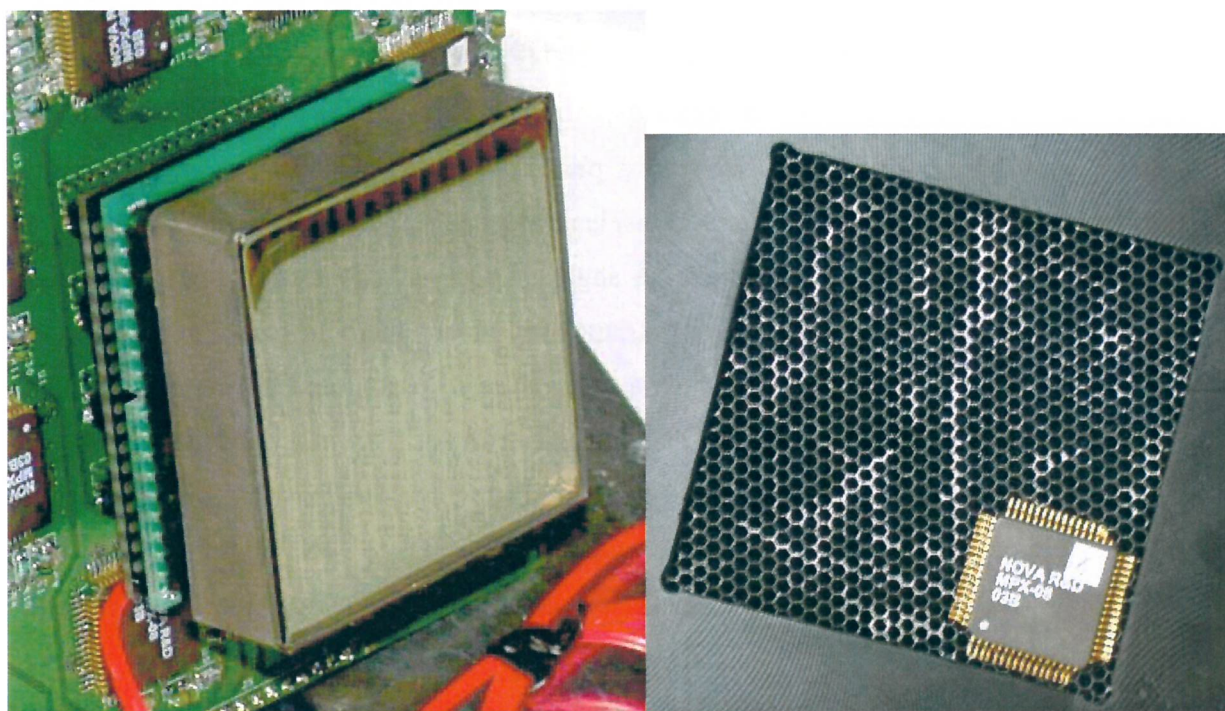


Figure 2. Left: A view of the H8500 PSPMT. Right: A view of the parallel hole collimator coupled with the H8500 PSPMT and the scintillator slab. Hexagonal holes have diameters of  $1.5\text{mm}$  or  $1.0\text{mm}$ . An MPX-08 chip is also shown.



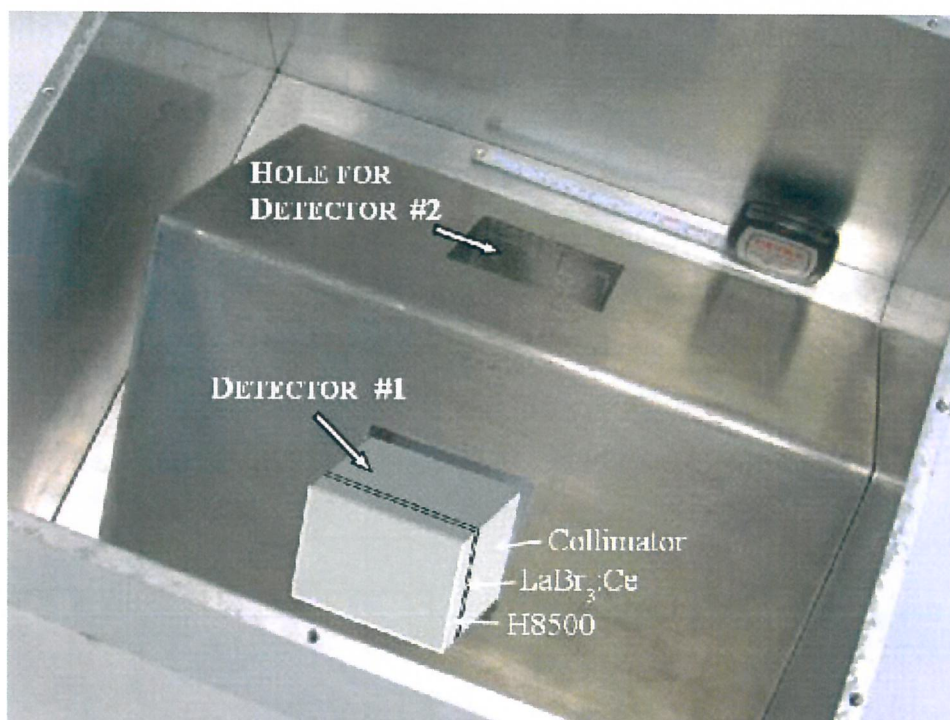


Figure 3. Top view of the triangular-shaped lead structure showing two holes for detectors housing. The mouse is placed on the bottom right and the detection system may rotate around it.



Figure 4. Bottom view of the structure, showing where the mouse is placed. Detectors face at 90°.

### III. The $\text{LaBr}_3\text{:Ce}$ scintillator

The new scintillation crystal  $\text{LaBr}_3\text{:Ce}$  shows very interesting properties (Table 1). The high light output at wavelengths suited for the bi-alkali photocathode (63000 light photons/MeV @ 380 nm), and the reduced non-proportionality with emitted photon energy (less than 5%) bring to a very good energy resolution (Figure 4). The extremely short scintillation decay time may in addition suggest the idea of an innovative PET device based on time of flight and a coincidence resolution time as low as 250ps [1].

Properties	NaI(Tl)	$\text{LaBr}_3\text{:Ce}$
Light yield (photons/keV)	41	63
Light output (% NaI(Tl) with bialkali PMT)	100	165
Wavelength at maximum emission	410	380
1/e decay time	230	16
Energy resolution ( $^{137}\text{Cs}$ )	5.6 %	2.8 %
Refractive index	1.85	1.9
Density	3.67	5.0

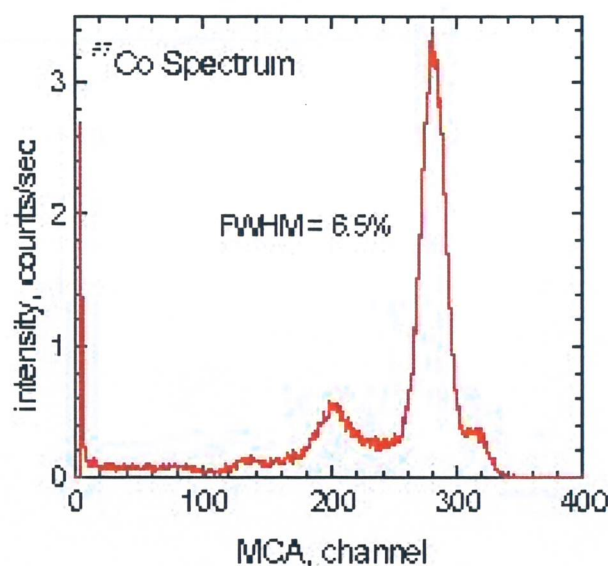


Figure 4. The energy resolution of  $\text{LaBr}_3\text{:Ce}$  is very high in comparison with other scintillator materials

Table. Summary of the  $\text{LaBr}_3\text{:Ce}$  properties in comparison with NaI(Tl) scintillator (source: Saint-Gobain)

#### IV. The MPX-08 chip

The MPX-08 integrated circuit is an eight-channel charge-integrating data acquisition system, suitable for measuring charges in the range from several fC to over 10 pC. It has been developed primarily for use with photomultiplier tubes and similar devices for measuring discrete charge pulse events.

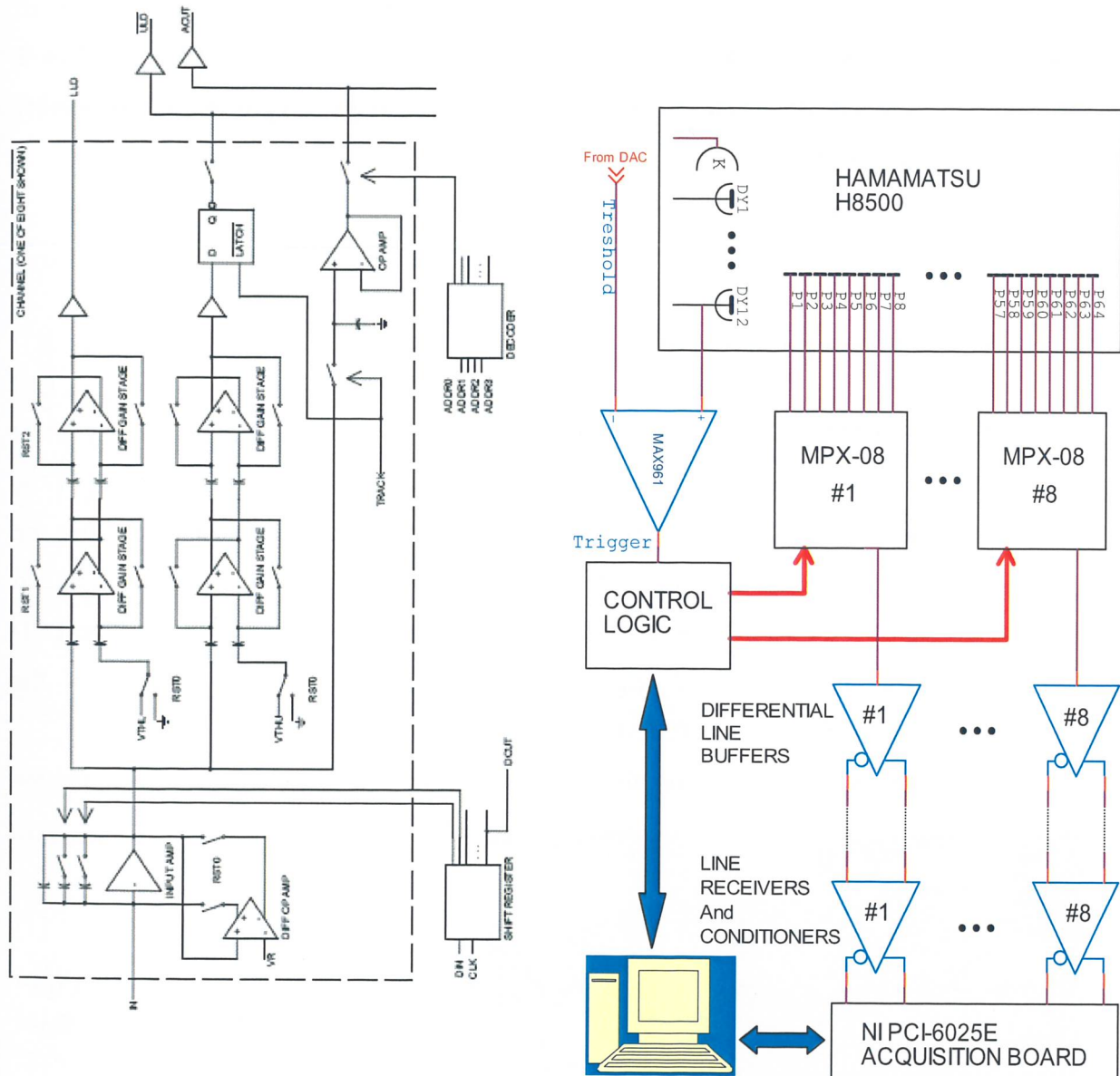


Figure 5. (LEFT) Block diagram of MPX-08 ASIC. (RIGHT) Block diagram of the electronics developed to acquire 64 signals from one H8500 PSPMP. The PCI-6025 board can acquire 16 differential channels, so the same board was used to reading both the PSPMT's.



The signal range is typically from 1 to 50 photoelectrons, assuming a nominal PMT gain of  $10^6$ . The MPX-08 is particularly well suited to minimize power in large pulse-mode detector systems.

A block diagram of the MPX-08 is shown in Figure 5 (left). Each channel includes a charge integrating input amplifier with variable gain, controlled from a binary word and two discriminators, the “lower level discriminator” (LLD) and the “upper level discriminator” (ULD). The charge-integrating amplifier outputs connect to transparent track/hold buffers, all controlled by a common TRACK signal. Readout of the latches and track/hold buffers is driven by the bits ADDR3÷ADDR0. Readout of the buffer stage can proceed independently from the operation of the input amplifier and discriminator stage.

The MPX-08 requires a power supply of 3.3V with a dissipation of 4.39mW.

## V. Conditioning and Acquisition electronics

The use of MX-08 ASIC as front-end electronics requires some logic circuitry to: 1) set the charge sensitive preamplifier gain; 2) set the integration time – as a function of the scintillator type and its eventual afterglow time; 3) discharge feedback capacitor after the pulse generation; 4) decode the serial output of each MPX-08; 5) address the eight ICs; and 6) generate the START CONVERSION pulses and the logic sequence to control the PCI-6025 acquisition board. In Fig.5 (right) is shown a simplified block diagram of the connections for one of the H8500 PSPMT.

The trigger signal comes from the 12<sup>th</sup> dynode of any H8500 and starts the acquisition of all the 64 signals.

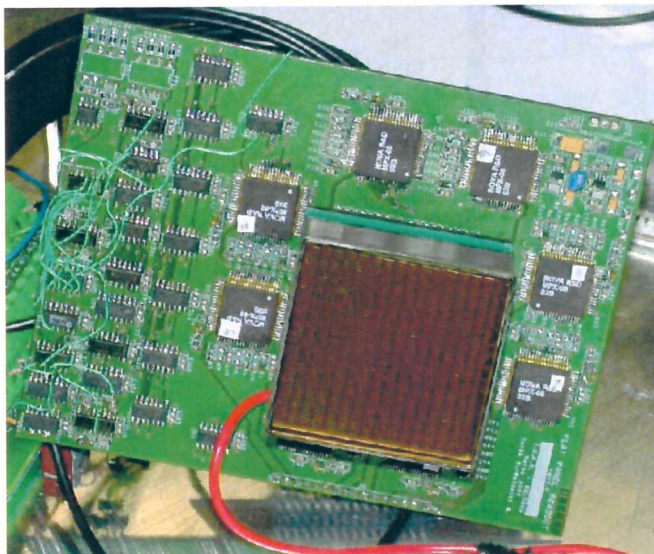


Figure 6. A prototype of the circuit board realized and tested. The H8500 PSPMT is surrounded by eight MPX-08 ASICs. In this board there is also the triggering circuitry and the control logic. The line buffers are housed on a piggy-back smaller board.

The output signals are converted into differential mode and transmitted to a receiver-conditioning stage for correcting differences in gain and offset, and performing a row equalization accounting for the anode non uniformity and the MPX-08 offset/gain tolerance. Finally the signals are converted to digits by the National Instruments PCI-6025 board. Any H8500 unit can acquire about 6000 events per second. Fig.6 shows a prototype board.

Figure 7 shows a raw spectrum, which was obtained with a  $^{57}\text{Co}$  source and the  $\text{LaBr}_3\text{:Ce}$  scintillator slab. The spectrum is the sum of the raw 64 channels before their fine equalization, which will be performed via software afterwards.

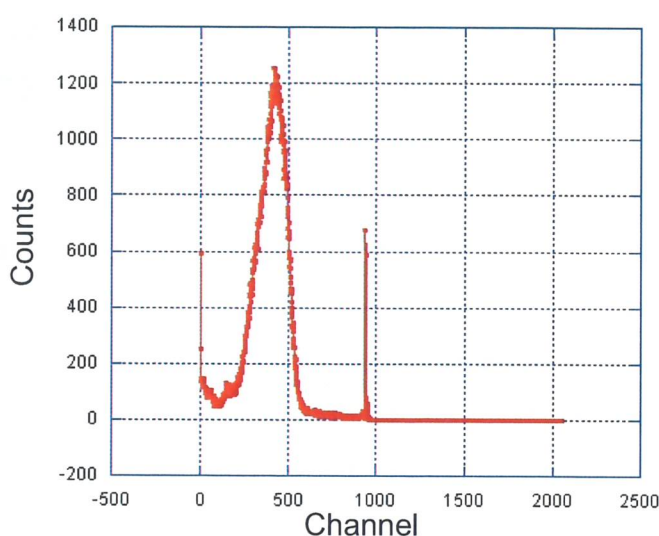


Figure 7. Raw spectrum of  $^{57}\text{Co}$  obtained with the prototype electronics.

## References

- [1] K. S. Shah, J. Glodo, M. Klugerman, W. W. Moses, S. E. Derenzo, and M. J. Weber,  $\text{LaBr}_3\text{:Ce}$  Scintillators for Gamma Ray Spectroscopy, *Submitted to IEEE Transactions on Nuclear Science*, LBNL-5179.
- [2] G. Visser, W. R. Binns, P. Dowkontt, P.L. Hink, R.M. Kippen, S. Kleinfelder, J. Macri, G.N. Pendleton, K. Rielage, T.O. Tumer, Design and performance of a low power integrated circuit readout system for multianode photomultiplier tubes, NOVA R & D Inc, Riverside, CA 92507, USA, [www.novarad.com](http://www.novarad.com).

## 2) STUDIES ON THE LABR3:CE SCINTILLATOR

### I. Introduction

Over the last years, there has been a growing interest in the development of a new class of fast scintillators like  $\text{LaCl}_3:\text{Ce}$  and  $\text{LaBr}_3:\text{Ce}$ . These new crystals are for the first time brighter than the  $\text{NaI}(\text{Tl})$  (49000/MeV and 63000/MeV @ bialkaly range for  $\text{LaCl}_3:\text{Ce}$  and  $\text{LaBr}_3:\text{Ce}$  respectively). In addition, their fast scintillation time (16 ns for  $\text{LaBr}_3:\text{Ce}$ ) is attractive as for SPECT and PET applications. Their most important feature is perhaps the excellent proportionality of the light yield to the gamma ray energy that may bring to an energy resolution nearly double as better (6-7% at 140 keV and 3% at 511 keV), which represents an absolute advance in the gamma ray imaging. Finally, these scintillators may in the long run become cost-effective and suitable for large detection areas, due to their low melting point (similarly to  $\text{NaI}(\text{Tl})$ ).

To assess their performance as nuclear medicine detectors, we have tested several continuous  $\text{LaBr}_3:\text{Ce}$  crystals with various sensible area, and thickness ranging between 4 mm and 10 mm. We also have compared them to  $\text{LaCl}_3:\text{Ce}$  continuous crystals and  $\text{NaI}(\text{Tl})$  crystals in continuous and pixilated configuration. The choice of the continuous configuration is due to limitations in the mechanical machining arising from fragility and higroscopicity of Lanthanum trialide crystal, in particular in pixilated configuration, which today limits the pitch to 4 mm. In any case, working with the basic principle of Anger camera for position determination, continuous crystals can offer the best position and energy resolution.

The scintillation crystals were coupled to a Hamamatsu H8500 Flat panel PSPMT, to evaluate the imaging performance, and to a standard PMT and SiAPD, to evaluate light output and energy resolution.



## II. Equipment and methods

Table I and II show scintillation and radiation properties of crystals.

TABLE I. CRYSTAL SCINTILLATION CHARACTERISTICS AT 140 keV

Crystal	$\rho$ (gr cm <sup>-2</sup> )	$\tau$ (cm <sup>-1</sup> )	$\mu$ (cm <sup>-1</sup> )	$\tau/\mu$	HVL (cm) @140keV	Thick. (cm) 80% efficiency
NaI:Tl	3.67	2.07	2.66	0.78	0.26	0.60
CsI:Tl	4.51	3.17	3.92	0.81	0.17	0.41
LaCl <sub>3</sub> :Ce	3.79	1.78	2.37	0.75	0.29	0.68
LaBr <sub>3</sub> :Ce	5.29	2.2	3.01	0.73	0.23	0.53

TABLE II. FURTHER CRYSTAL SCINTILLATION PROPERTIES

Crystal	Light yield (ph/keV)	Decay time (ns)	Maximum Emission (nm)	$\Delta E/E$ (FWHM) (%) PMT read-out	
				662 keV**	140 keV
NaI:Tl	41	230	410	5.6	8.5
CsI:Tl	66	$8 \div 6 \times 10^5$	550	6.6	14
LaCl <sub>3</sub> :Ce	49	28	350	3.8	8.0
LaBr <sub>3</sub> :Ce	63	16	380	2.8	5.8
** from C.W.E. van Eijk Phys. Med. Biol. (2002) 85-106					

Three  $\text{LaBr}_3\text{:Ce}$  continuous crystals have been specifically designed and coupled to Flat Panel PMT H8500 (PSPMT) for position sensitive measurements. The first one  $\text{LaBr}_3\text{:Ce}$  crystal,  $50 \times 50 \times 5 \text{ mm}^3$ , has been “integral” assembled with the PSPMT. This detector configuration permits both the narrowest light distribution and the highest light collection to obtain the best spatial and energy resolutions respectively. At the same time, 5 mm crystal thickness allows 80 % efficiency at photon energy of 140 keV. The other two  $\text{LaBr}_3\text{:Ce}$  crystals,  $50 \times 50 \text{ mm}^2$  area, were coupled to a PSPMT through an optical glass window 3 mm thick; being this window necessary to cope with the high higroscopicity of the crystal. In order to minimize the distance between photon interaction point and photocathode, the thickness of one of the crystals was reduced to 4 mm; consequently a detection efficiency of 70% at 140 keV was expected. The planar 10 mm thick  $\text{LaBr}_3\text{:Ce}$  has been chosen for its high efficiency (up to 95 %, @140 keV). The back surfaces of the crystals were grinded with certain grit and covered with white diffusive reflector to obtain the highest light output. A black light absorber was placed on edges to avoid position distortions due to light reflections. The fourth  $\text{LaBr}_3\text{:Ce}$  of one inch diameter and thickness was only used to measure the light output and the energy resolution. This crystal was the first sample of  $\text{LaBr}_3\text{:Ce}$  made by Saint Gobain (2003), and was explicitly designed to enhance the spectrometric response. Figure 1 shows the integral line  $\text{LaBr}_3\text{:Ce}$  detector and the 10 mm  $\text{LaBr}_3\text{:Ce}$  detector with housing.



Figure 1. *On the left: of integral line  $\text{LaBr}_3\text{:Ce}$  detector. On the right: picture of 10 mm  $\text{LaBr}_3\text{:Ce}$  detector with housing.*

The  $\text{LaBr}_3\text{:Ce}$  has been compared to three  $\text{LaCl}_3\text{:Ce}$  continuous crystals (area=1 square inch) coupled to PSPMTs. Two of them, 3 and 6 mm thick respectively, have been coupled through a 3 mm thick glass window (because of the material higroscopicity). The third, 3 mm thick, has been integral assembled with a one inch PSPMT Hamamatsu R5900-

C8 [1] in order to highlight spatial and energy resolution response. Surface treatment was the same described previously for LaBr<sub>3</sub>:Ce.

Finally, a further comparison have been carried out also with a NaI(Tl) continuous crystal, 1.5 mm thick, integral assembled with the PMT H8500 [2]. This latter configuration is a good trade-off between spatial resolution and detection efficiency.

Table III summarizes the crystals configurations, where “Integral” means “integral assembled with the PSPMT” and “regular” indicates the presence of a crystal glass window. The H8500 [3] was plugged to a 64 channel read out, developed by the Southampton University. Each channel consists of preamplifier, sample and hold and multiplexer. Finally the read-out goes to a National Instruments ADC AT-MIO 6110 card [4, 5], as in Figure 2.

We have measured the energy resolution with a standard 3” PMT Thorn EMI 9765B05 (29 % photocathode quantum efficiency) connected to a spectrometric chain, and also with a Hamamatsu S8664-55 Si-APD. The APD has overall dimensions 10.6x9.0mm<sup>2</sup> with 5x5mm<sup>2</sup> active area, on which a thin (0.45mm) epoxy resin is deposited [6].

We have employed free and collimated point radioactive sources to evaluate the energy resolution, and scanned these sources along the crystal to measure spatial resolution and position response. According to the Anger principle, measurements have aimed at determining charge distribution spread, position linearity, spatial resolution, and energy resolution.

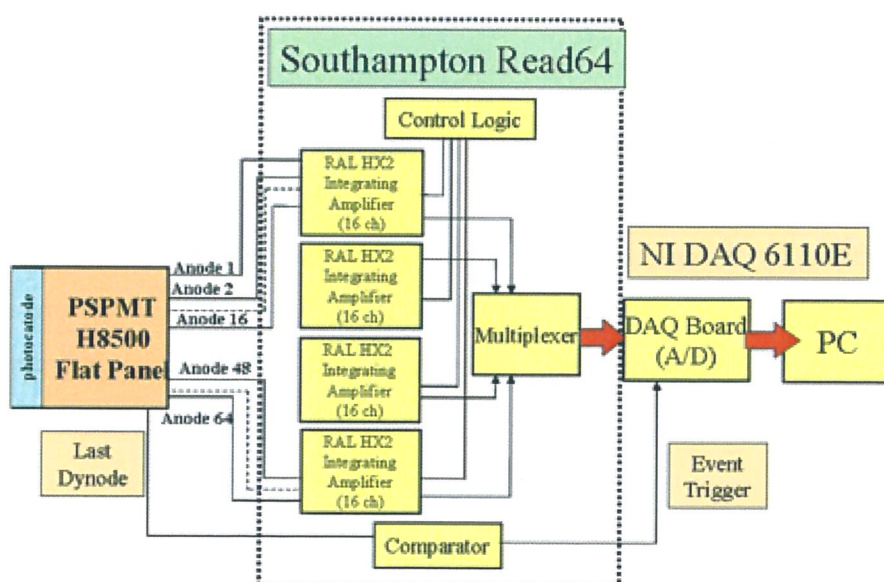


Figure 2. Sketch of 64 channels system readout.



TABLE III  
SCINTILLATOR CRYSTAL

Crystal	Type	Size (mm <sup>2</sup> )	Thickness (mm)	Optical Window (mm)	Assembly
La Cl <sub>3</sub> :Ce	planar	25x25	3	-	Integral with R5900-C8 PSPMT
La Cl <sub>3</sub> :Ce	planar	25x25	3	3	Regular
La Cl <sub>3</sub> :Ce	planar	25x25	6	3	Regular
LaBr <sub>3</sub> :Ce	planar	50x50	4	3	Regular
LaBr <sub>3</sub> :Ce	planar	50x50	10	3	Regular
LaBr <sub>3</sub> :Ce	planar	12.7 mm Ø	12.7	5	Regular
LaBr <sub>3</sub> :Ce	planar	50x50	5	-	Integral with H8500 FP-PMT
NaI:Tl	planar	50x50	1.5	-	Integral with H8500 FP-PMT

### III Results. Spectrometric measurements

We started by doing a crystal scanning of a Co<sup>57</sup> sources, collimated by a 2 mm aperture. The crystals were coupled to a standard PMT. The results of this investigation are shown in figure 3, for LaBr<sub>3</sub>:Ce planar, 12.7 mm Ø, and 12.7 mm thick in comparison with continuous LaCl<sub>3</sub>:Ce crystals.

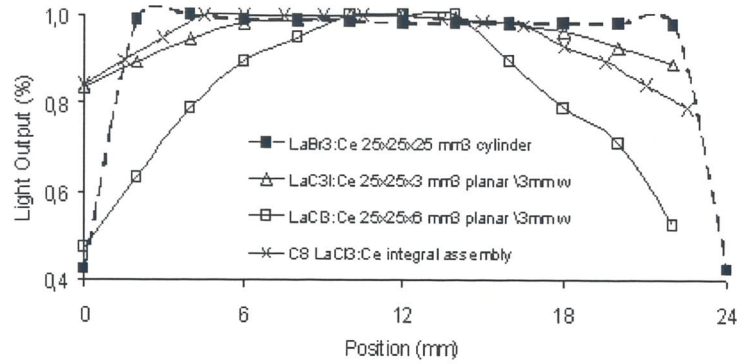


Figure 3. Light output resulted by crystal scanning with a collimated  $\text{Co}^{57}$  source.

The results show a decreasing of light output from the centre to the edges, ranging between 20% and 50% for 3 mm and 6 mm thickness respectively, due to the suboptimal light collection. Taking into account only the maximum light output measured in the centre of crystal and considering the different light yield of the two materials, we would estimate an overall light loss of about 50% and 60% for  $\text{LaBr}_3:\text{Ce}$  and  $\text{LaCl}_3:\text{Ce}$  respectively.

The energy resolution results obtained with standard PMT and SiAPD are summarized in figure 4. There is a small difference between continuous  $\text{LaBr}_3:\text{Ce}$  crystal, 4 mm thick, and the 1" crystal with the best light collection. Moreover, the  $\text{LaBr}_3:\text{Ce}$  crystal performs better than  $\text{NaI}(\text{Tl})$  and  $\text{LaCl}_3:\text{Ce}$  in the energy range involved in nuclear imaging ( $\Delta E/E=0.06$  at 140 keV). Figure 5 shows some pulse height distributions.

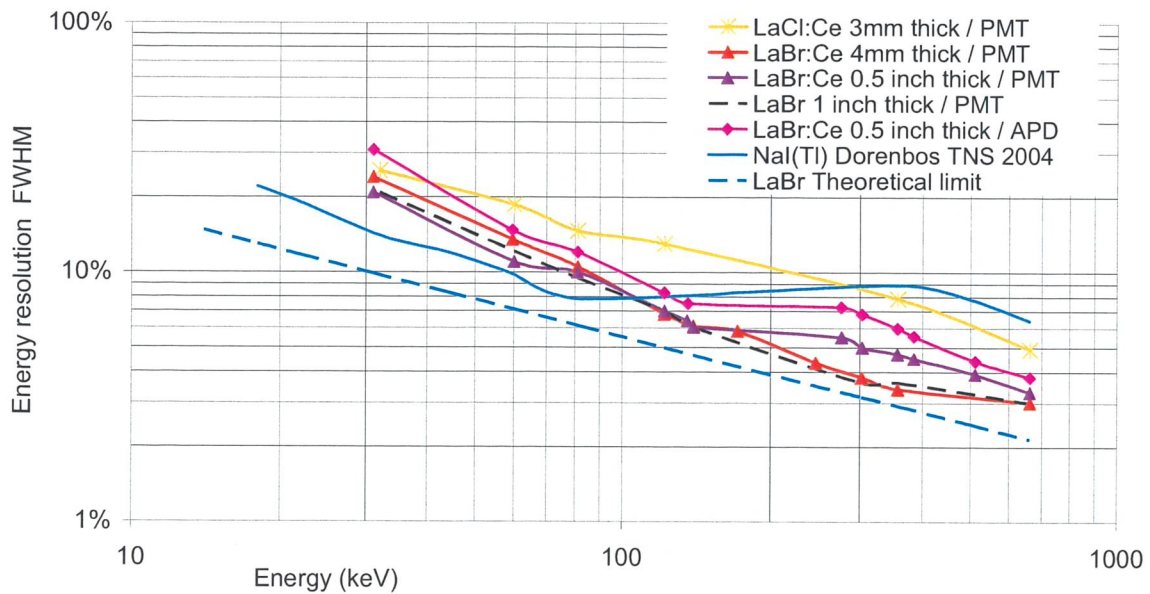


Figure 4. Energy resolution of different crystals and configuration.

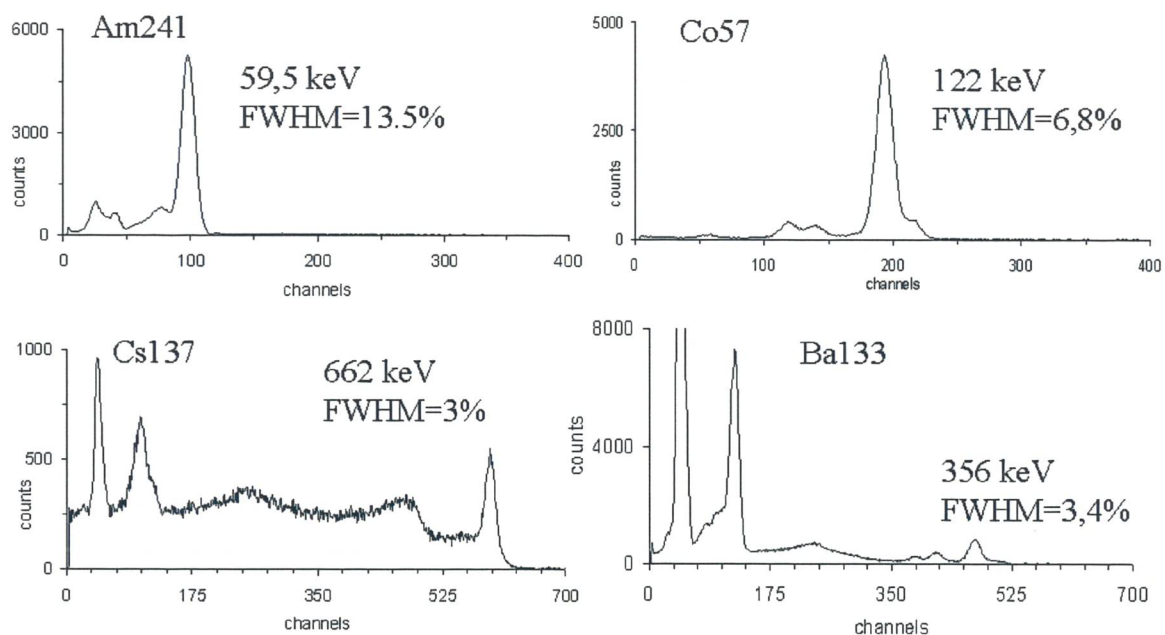


Figure 5. Pulse height distributions for 4mm thick  $\text{LaBr}_3:\text{Ce}$  continuous crystal coupled to standard PMT.

#### IV. Results. Positioning performances

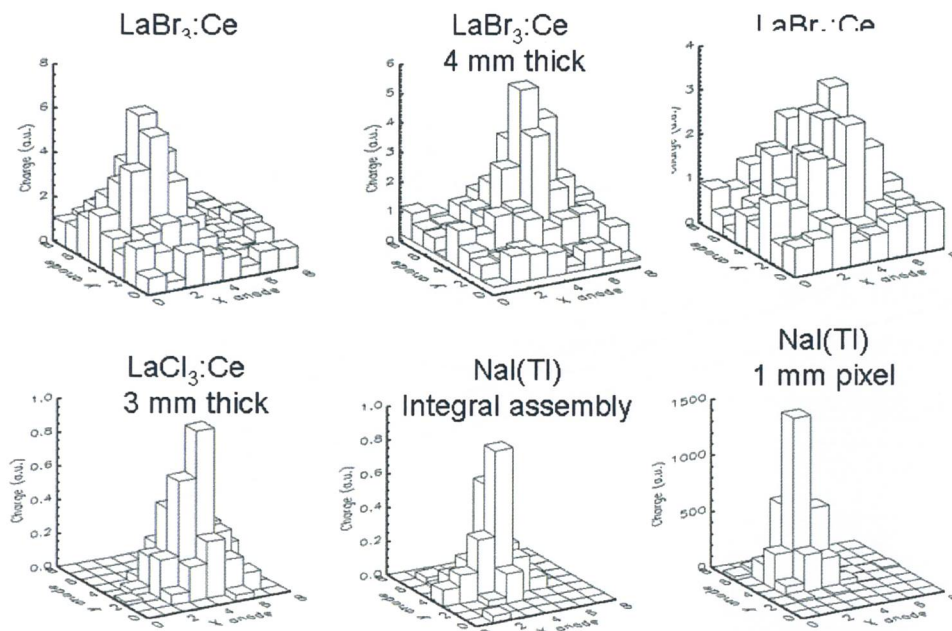


Figure 6. Charge distribution on anodic plane of H8500 PSPMT for all investigated crystals.



We have evaluated that the charge spread FWHM was ranging from 12 mm to 18 mm for integral assembly and 10 mm thick LaBr<sub>3</sub>:Ce crystal respectively (Figure 6 shows some instances). The NaI(Tl) integral assembly detector shows a narrower charge distribution (10 mm), mainly for the smallest thickness, but in any case close to the LaBr<sub>3</sub>:Ce integral assembly behavior.

From the charge distribution we can evaluate the expected spatial resolution by the formula:

$$SR = ER \times \sigma_{\text{charge\_distrib}}$$

where ER is the Energy Resolution, and  $\sigma_{\text{charge\_distrib}}$  is the charge distribution FWHM. This formula was obtained starting from the position centroid formula, i.e. for x direction:

$$X_c = \frac{\sum_j n_j x_j}{\sum_j n_j}$$

and taking into consideration the point spread function and the Poisson statistics.

Figure 7 shows the calculated spatial resolution vs. the mechanical position, for 5 and 10 mm LaBr<sub>3</sub>:Ce continuous crystal, in comparison to the smallest thickness crystal produced by Saint Gobain at this moment (1.5 mm). The detection area was 50 mm<sup>2</sup>. The curves are obtained from the depth of interaction, and the behavior of the light collection at the crystal edges.

All crystals show a wide range of constant response in the central zone and a slight worsening at the edges, due to the truncation of the charge distribution. Anyway, the expected active range with uniform response is 36 and 42 mm with a spatial resolution of 0.7 mm and 1.9 mm, for 5 and 10 mm LaBr<sub>3</sub>:Ce crystal respectively.

To confirm these results, the position linearity and energy resolution were evaluated by a 1.5 mm step scanning of the crystals with 1mm Co<sup>57</sup> collimated source.

In figure 8, we show the position linearity for 10 mm and integral assembly LaBr<sub>3</sub>:Ce crystal in comparison with NaI(Tl) integral assembly crystal. For integral assembly configuration, the LaBr<sub>3</sub>:Ce behaves closely to what we calculated and the range of position uniformity is ~36 mm. For the 10 mm thick the result is slightly worse than calculated, probably because we did not take into account the reflection of light at the surfaces.

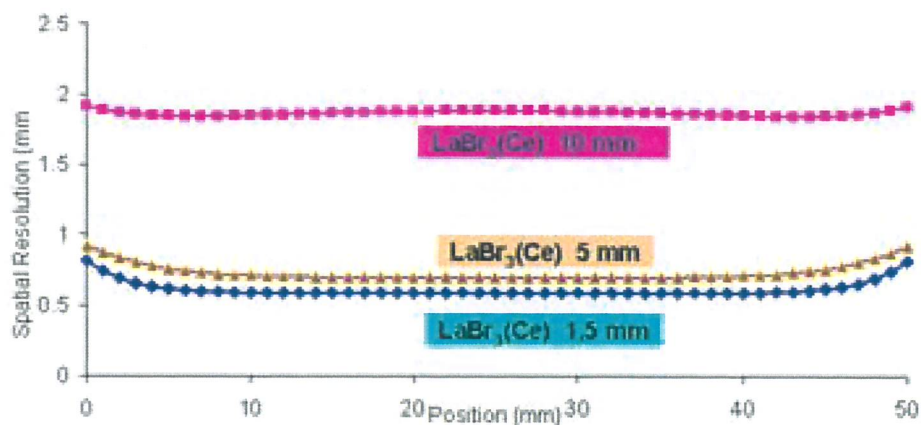


Figure 7. Calculated spatial resolution vs. mechanical position for 1.5, 5 and 10 mm  $\text{LaBr}_3\text{:Ce}$  continuous crystal.

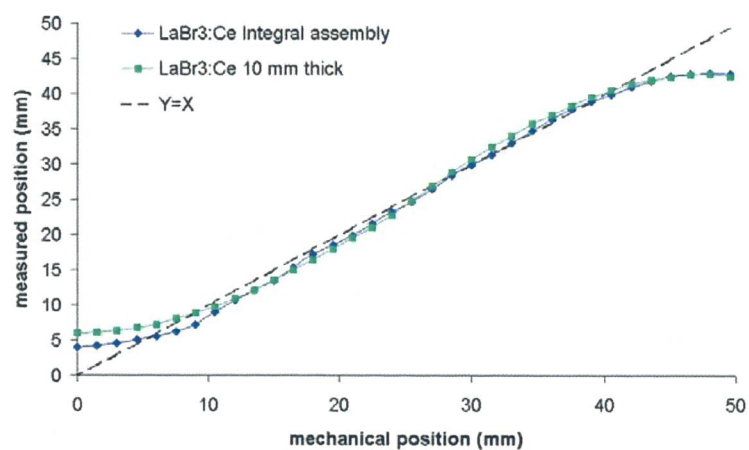


Figure 8. Position linearity obtained by scanning with a collimated  $\text{Co57}$  source of 10mm and integral assembly  $\text{LaBr}_3\text{:Ce}$  crystal.

In Figure 9 the images and scanning profiles of the three  $\text{LaBr}_3\text{:Ce}$  crystal are shown. The inset also reports the intrinsic spatial resolution. The best value obtained is 0.9 mm for the integral assembly detector, demonstrating that this configuration is optimal for imaging. However, also the 1.85 mm value of the 10 mm thick crystal is an important result for imaging applications where high detection efficiency is required.

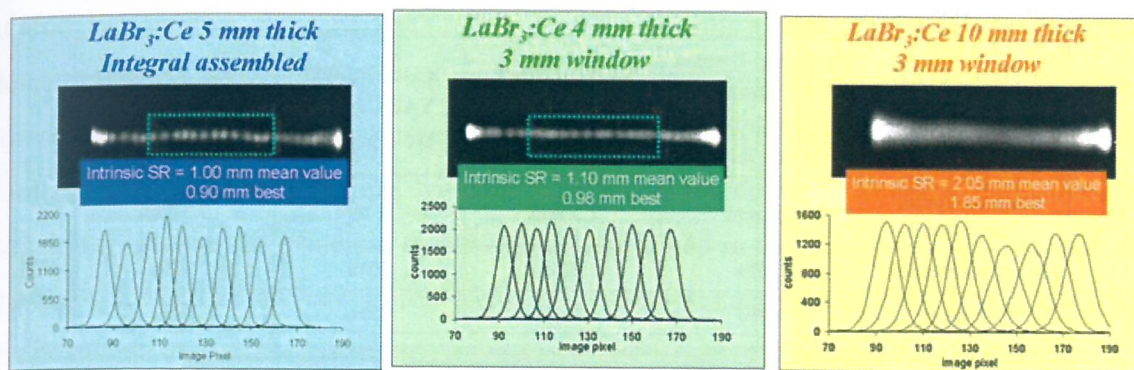


Figure 9. Image and relative profiles of spots scanning at 1.5 mm step performed with 1 mm collimated Co<sup>57</sup> for the three LaBr<sub>3</sub>:Ce crystals.

We have compared the LaBr<sub>3</sub>:Ce integral assembly detector to three gamma cameras of the previous generation: a 3" camera based on Hamamatsu R2486 PSPMT coupled to CsI(Tl) pixilated crystal 1.2 mm pitch, the YAP gamma camera (pixellated crystal 0.6 mm pitch), and a standard Anger Camera. The test was performed acquiring absorption images of lead radiological objects, utilizing a Co<sup>57</sup> point source at 150 cm from the test object. The mask consisted of four lead (1.90±0.03 mm thick) numbers ("0", "4", "7", "1") arranged on a thin acetate sheet so as to cover an area of roughly 2×2 cm<sup>2</sup>. The mask and the relative images are shown in figure 10. Please, note that images with similar contrast do not correspond to detectors with similar efficiency, like for LaBr<sub>3</sub>:Ce and YAP detector. The contrast for the image obtained by LaBr<sub>3</sub>:Ce detector was 84%

Finally, Figure 11 compares the Modulation Transfer Functions of the integral assembly LaBr<sub>3</sub>:Ce detector, and NaI(Tl) 1 mm pixilated crystal, coupled to H8500 FP-PMT. The MTF curves are obtained as Fourier transform of a linear source, i.e. a capillary, 0.5 mm ID, filled with Tc<sup>99m</sup>, in front of a General Purpose Collimator (1.5 mm hole, 0.2mm septa, 22 mm thick). In addition, we plotted the result of a Monte Carlo simulation of the collimator response to the capillary. The lanthanum MTF is very close to the simulated MTF of the collimator, which represents the upper limit for the considered experimental detector configuration. Also the figure shows that the lanthanum performs better than the NaI(Tl) pixilated crystal, in term of spatial resolution and image contrast.



Gamma Camera & Crystals	<u>Lanthanum Gamma Camera</u> LaBr <sub>3</sub> :Ce planar (5 mm thick)	R2486 PSPMT CsI(Tl) array 1.2 mm pitch	R2486 PSPMT YAP:Ce array 0.6 mm pixel	<u>ANGER Camera</u> NaI(Tl) planar (6 mm thick)
Intrinsic Spatial Resolution*	0.9 mm	1.3 mm	1.1 mm	3.5 mm
Energy Resolution*	6.5%	23%	50%	10%
Efficiency*	80%	40%	45%	80%



Figure 10. Lead radiological object – Absorption images. The lead mask is shown on the left. Note that the YPP imaged a mask with larger distance between the numbers in the mask.

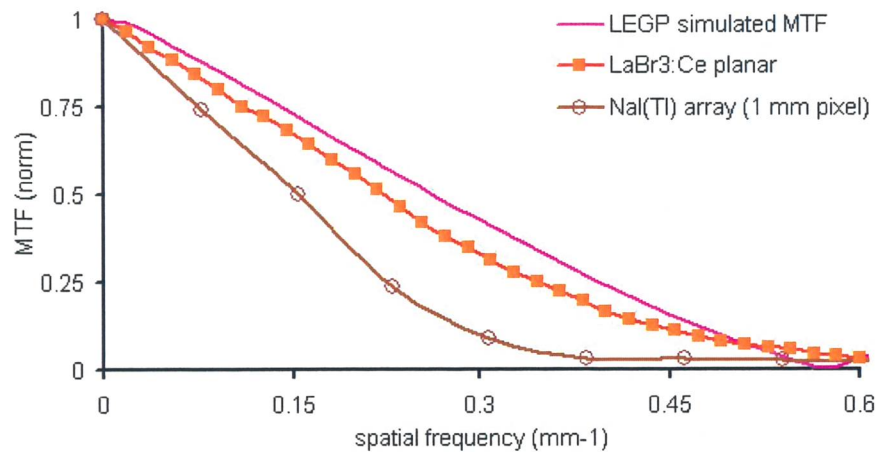


Figure 11. MTF of the integral assembly Labr3detector, the NaI(Tl) 1 mm pixellated crystal, coupled to H8500 FP-PMT, and the Monte Carlo simulation of a collimator.

## V. Conclusion

In conclusion, the LaBr<sub>3</sub>:Ce continuous crystal shows a very good spatial resolution even with high crystal thickness ( 1 cm) and additional glass window. It demonstrated very good optical properties for position sensitive measurements, with intrinsic spatial resolution up to 0.9 mm FWHM, and is extremely attractive as for the energy resolution of 6% obtained

at 140 keV with a standard PMT. This crystal performs better than previous generation detectors based on NaI(Tl) [7] or the recent LaCl<sub>3</sub>:Ce continuous crystal [8]. We easily foresee for the near future further improvements that will bring inorganic scintillation cameras to a close competition with the semiconductor devices. Already, from table IV, which summarizes the principal results we have obtained in this study, we can conclude that the LaBr<sub>3</sub>:Ce continuous crystal represents today the best candidate to replace the NaI(Tl) for the new generation of gamma ray imaging detectors.

TABLE IV  
PRINCIPAL RESULTS

Detector	FP NaI:Tl planar	FP LaCl <sub>3</sub> :Ce planar	R5900-C8 LaCl <sub>3</sub> :Ce planar	FP LaBr <sub>3</sub> :Ce planar	FP LaBr <sub>3</sub> :Ce planar	FP LaBr <sub>3</sub> :Ce planar
Optical Guide (mm)	Integral assembly	3	Integral assembly	Integral assembly	3	3
Crystal Thick (mm)	1.5	3	3	5	4	10
Intrinsic Spatial Resolution (FWHM mm)	0.8	1.3	1.0	0.9	1.1	1.9
Charge Spread (FWHM mm)	10	16	12	12	16	18
Energy Resolution @140 keV -FWHM % (including PSPMT)	10	13	15	7.5%	7.5%	12%
Efficiency % Energy window	28	42	42	80	70	95

## Bibliography

1. Hamamatsu Technical Data Sheet Position Sensitive Photomultiplier Tube R5900U-OO-C8 Preliminary, printed in Japan, December 1995
2. Cinti M.N., IEEE member, Majewski S., Williams M.B., Bachmann C., Cominelli F., Kundu B.K., Stolin.A., Popov V., Welch B.L., DeVincentis G., Betti M., Ridolfi S. and Pani R, "Iodine 125 imaging in mice using NaI(Tl)/Flat panel PMT integral assembly", Nuclear Science, IEEE Transactions on, in press
3. Hamamatsu Photonics K.K., "H8500 series data sheet", .2005 DN, Japan
4. "HX2/RAL/SS System Readout", Rutherford, Applet on Labs Microelectron Group, Tech. Data Sheet, Chilton-Didcot, Oxfordshire UK, 1995
5. P Pani, R. Pellegrini, M.N.Cinti, C.Trotta, P.Bennati, F Cusanno, F. Garibaldi, "Imaging detector design based on flat panel PMT", Nucl. Instr. Meth. Sect. A, Vol. 527, 2004, pp. 54- 57
6. Hamamatsu Photonics K.K., "Si APD S8664 series data sheet", Sep.2005 DN, Japan
7. Cinti M.N., IEEE member, Majewski S., Williams M.B., Bachmann C., Cominelli F., Kundu B.K., Stolin.A., Popov V., Welch B.L., DeVincentis G., Betti M., Ridolfi S. and Pani R., IEEE member, "Iodine 125 imaging in mice using NaI(Tl)/Flat panel PMT integral assembly", Nuclear Science, IEEE Transactions on , in press
8. Pani R., Cinti MN., De Notaristefani F., Pellegrini R., Bennati P, Betti M., G. Trotta., Karimian A.,Mattioli M., Garibaldi F., Cusanno F. and Orsolini Cancelli V. "Imaging performances of LaCl<sub>3</sub>:Ce scintillation crystals in SPECT", Nuclear Science, IEEE Transactions on, in press.
9. Pani R., Cinti M. N., Pellegrini R., De Notaristefani F., Bennati P., Betti M.,Trotta G., Mattioli M., Garibaldi F., Orsolini Cancelli V., Moschini G., and Navarria F.," LaBr<sub>3</sub>:Ce scintillation camera", IEEE Nuclear Science Symposium Conference Record, Volume 4, 23-29 Oct. 2005 Page(s):2061 - 2065



## 2) MEASURING THE IMAGED-OBJECT DISTANCE WITH A STATIONARY HIGH-SPATIAL-RESOLUTION SCINTILLATION CAMERA

(Patent No RM 2006 A 000216, UIBM Roma)

### **Abstract**

*A method to measure the detector-to-object distance from the images obtained with stationary high-spatial-resolution gamma-ray cameras for in vivo studies has been developed. It exploits the shift of the imaged object in the image plane, obtained at a certain tilt of the parallel-hole collimator. A linear dependence of the image displacement on the distance to the object has been measured using a high-spatial-resolution scintillation camera employing an yttrium–aluminium perovskite (YAP) scintillator. It is shown that the modified YAP camera can be used to obtain three-dimensional information without moving the camera or the object. The method could be applied in scintimammography and radioguided surgery, in lymphoscintigraphy, as well as in the analysis of the biodistribution of radiopharmaceuticals.*

**Keywords:** Imaging, position-sensitive detector, scintimammography, radioguided surgery, lymphoscintigraphy, bulk-material analysis

### **I. Introduction**

At present the complete three-dimensional object imaging can be achieved by using array-detector systems [1-3]. For practical purposes however, it is desirable to have an imaging system with high spatial resolution combined with a good sensitivity and compact dimensions. One way to achieve this is to use compact small-area single-photon detectors positioned as close as possible to small-body regions thus making advantage of the larger solid angle combined with the single photon detection sensitivity. Two-dimensional plane scintigraphic detectors are exploited in order to image small superficial lesions of the tissues or organs [4, 5]. However it would be desirable to extend these diagnostic possibilities by detecting the objects of interest in somewhat larger depth.

We present a method to simultaneously image the object and determine its distance from the detector. The advantage of the method is that it is not necessary to move the camera at different angles or to turn the object around its axes.

## II. Determining the scintillator-to-object distance

A simple way to determine the distance from the scintillator to the imaged object is to use the shift of the image when the parallel-hole lead collimator of the camera is tilted by a certain angle. In Figure 1(a) and Figure 1(b) are schematically presented the images obtained from point-like sources  $S_1$ ,  $S_2$  and  $S_3$ , situated on an axis perpendicular to the scintillator  $Sc$  and placed at different distances  $z_1$ ,  $z_2$  and  $z_3$  from it, respectively. In Figure 1(a) the parallel-hole collimator of the camera  $C$  is parallel to the scintillator  $Sc$  and in Figure 1(b) the collimator is tilted by an angle  $\varphi_1$  ( $\varphi_2$  for the opposite direction, represented by a broken line) around an axis parallel to the scintillator surface.

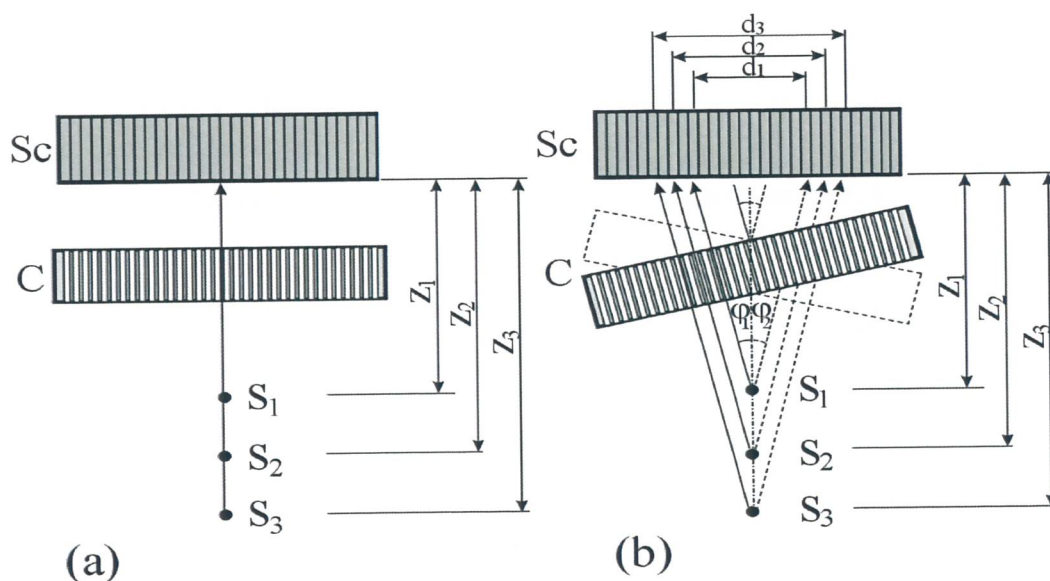


Figure 1. Schematic representation of the image positions from three point-like sources  $S_1$ ,  $S_2$  and  $S_3$  at distances  $z_1$ ,  $z_2$  and  $z_3$  from the scintillator plane respectively. In Figure 1(a) the parallel-hole collimator  $C$  is parallel to the scintillator plane. In Figure. 1(b) the parallel-hole collimator is tilted by an angle  $\varphi_1$  ( $\varphi_2$  for the opposite direction, represented by a broken line) around an axis parallel to the scintillator surface.

In Figure 1(a) it is evident that the images of the three point-like sources are coincident. Because of the properties of the parallel-hole collimator to transmit the gamma-

rays perpendicular to its surface, the images in Figure 1(b) are shifted by different values. The length of the shift is proportional to the source-to-scintillator distance and to the collimator tilt angle.

From the images corresponding to the two angular positions of the parallel-hole collimator one can extract the total source position shift. It depends on the object distance ( $z$ ) and the two tilt angles ( $\varphi_1$  and  $\varphi_2$ ) according to:

$$d_i = z_i (tg(\varphi_1) + tg(\varphi_2)); (i=1, 2, 3), \quad (1)$$

where  $\varphi_1$  and  $\varphi_2$  are the absolute values of the two opposite tilt angles of the parallel-hole collimator (Figure 1(b)).

For known values of  $d_i$ ,  $\varphi_1$  and  $\varphi_2$ , by inverting (1) with respect to  $z$ , one can obtain the required scintillator-to-object distance.

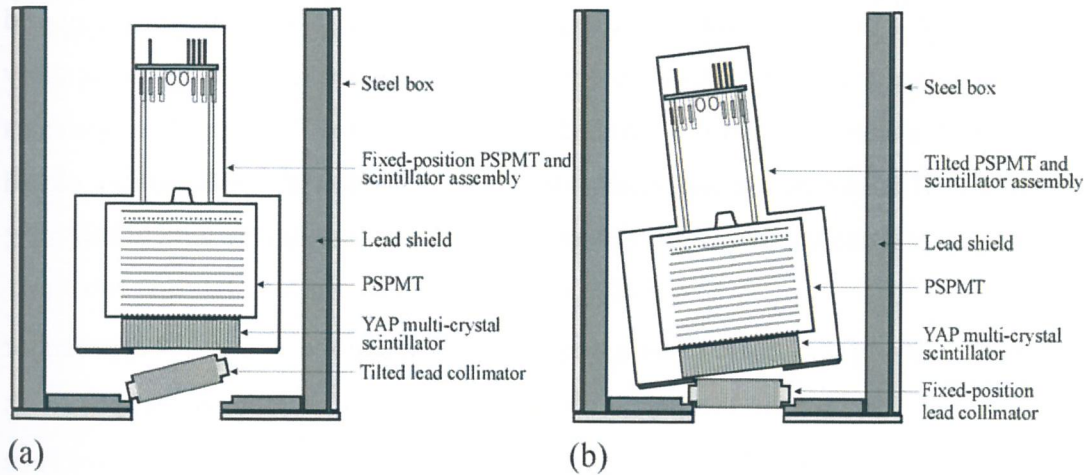


Figure 2. A schematic representation of the two possible measurement setups: (a) a setup with a fixed scintillator-PSPMT assembly and tilted parallel-hole collimator; (b) a setup with a fixed parallel-hole collimator and tilted scintillator-PSPMT assembly.

The oblique collimator measurements can be performed using either one of the two different setups shown in Figure 2(a) and Figure 2(b). In the first setup the parallel-hole collimator can be tilted with respect to the fixed-position scintillator and position-sensitive photomultiplier tube (PSPMT) assembly. In the second setup the PSPMT and scintillator assembly can be tilted with respect to the fixed-position collimator.

The method described above is valid for all the available position-sensitive imaging detectors.



### III. Experimental check of the method

The method for measuring the scintillator-to-object distance was checked using the first setup (Figure 2(a)) by modifying the Cerium-doped Yttrium-Aluminum Perovskite scintillation camera (YAP:Ce) used for small animal imaging [6]. It has an effective area with a diameter of 50mm. The lead collimator, placed in front of the scintillator, has a shape of parallelepiped (40mm x 40mm x 20mm). The parallel collimator holes with diameter of 0.5mm are situated at a distance of 0.65mm. The gamma-camera FOV is 40 x 40 mm. The collimator was placed in a cradle-like support ensuring maximum tilt angles  $\varphi_1=5.5^\circ$  and  $\varphi_2=-5.5^\circ$  around a horizontal axis.

To determine the dependence of the image shift (d) on the distance to the imaged object we have used a horizontal glass capillary tube filled with  $^{99m}\text{Tc}$  solution and placed parallel to the scintillator plane at a distance  $z$  from the camera entrance. The glass capillary tube had internal diameter less than 0.7 mm and a length of 11cm. To ensure homogeneous distribution of the  $^{99m}\text{Tc}$  during the experiments the capillary tube was connected to a closed circuit including a peristaltic pump keeping continuous liquid circulation with a flux of 2  $\text{cm}^3/\text{min}$ .

The uniformity of the YAP camera response was measured using  $^{99m}\text{Tc}$  generator eluate for the three positions of the parallel-hole collimator:  $\varphi_1=0^\circ$  (horizontal position);  $\varphi_1=5.5^\circ$  and  $\varphi_2=-5.5^\circ$ . Following the procedure described in [6] correction matrices have been generated for the three positions of the collimator. For each collimator position the corresponding correction matrix was applied to the acquired image to compensate for the camera nonuniformities.

Measurements of the image shift have been made using horizontally placed capillary tube, for several capillary-to-camera distances and two positions of the parallel-hole collimator ( $\varphi_1=5.5^\circ$  and  $\varphi_2=-5.5^\circ$ ). The capillary tube was placed parallel to the collimator tilt axis. Images have been collected with a minimum amount of  $2 \times 10^6$  counts in the FOV. The maximum values of the count-rate did not exceed  $500\text{s}^{-1}$ . After the homogeneity correction, the positions of the selected regions from the capillary-tube image have been obtained. The count distributions from selected slices of the capillary-tube images for each collimator position have been obtained. The shifts between the peak centroids for the images corresponding to equal  $z$  have been measured. In Figure 3 are shown the count distributions

obtained for 18mm camera-to-capillary distance and for the two angular positions of the parallel-hole collimator.

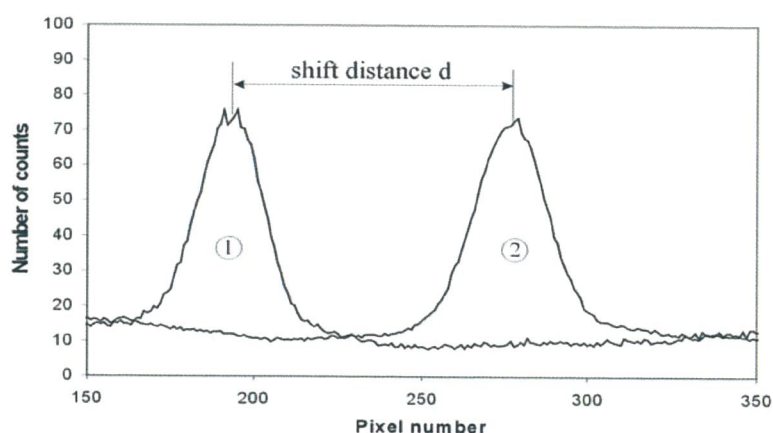


Figure 3. Image shift of a horizontal capillary tube placed at distance of 18 mm from the YAP camera. Peaks 1 and 2 correspond to collimator tilt angles  $\phi_1=5.5^\circ$  and  $\phi_2=-5.5^\circ$ .

The shifts of the capillary-tube images are plotted in Figure 4. The values for the peak shift distance  $d$  show fairly good linear dependence on the camera-to object distance. The evaluated correlation coefficient is  $r=0.998 \pm 0.005$ .

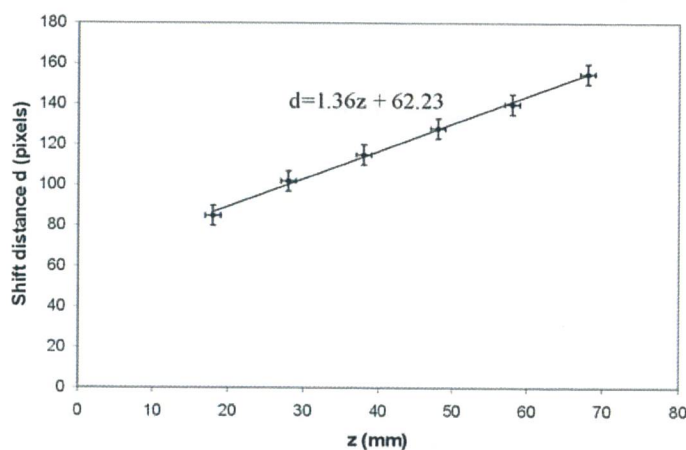


Figure 4. Capillary-tube image shift  $d$  versus camera-to-capillary distance  $z$ , measured for the two tilt angles of the parallel-hole collimator. The parameters of the linear least-squares fit to the experimental values are shown in the Figure.

#### IV. Applications

The results obtained confirm the possibility to measure the distance from the camera to the object. The measured distance error depends on the spatial resolution of the camera and on the collimator tilt angle. Higher spatial resolution implies smaller error in object localization in the image plane. Larger tilt angles yield increased peak-shift distances which in turn reduce the relative error in z-coordinate determination. For given camera-to-object distance the full width at half maximum of the capillary-tube image was found to be independent of tilt angle, which means that the system resolution is not affected by the oblique-collimator measurements.

The obtained results give us the possibility to introduce the third coordinate ( $z$ ) in the images reconstruction, provided that well-defined image shifts could be tracked on the image plane.

The method can be applied in medical applications such as: localizing non-palpable cancer (with size smaller than 1cm) in scintimammography as well as in lymphoscintigraphy for localizing and characterizing lymph nodes, in radioguided surgery and in all cases when localizing the position of the gamma-ray emitting objects is crucial. In addition the method can be exploited for *in-vivo* analysis of biodistributions of radiofarmaceuticals, as well as in complex structure gamma-ray imaging and bulk-material defect analysis.

#### References

- [1] J. L. Humm, A. Rosenfeld, A. Del Guerra, From PET detectors to PET scanners, Eur. J. Nucl. Med. Mol. Imaging, Vol 30, No 11 (2003), pp 1574 - 1597
- [2] N. K. Doshi, R. W. Silverman, Y. Shao, S. H. Cherry, maxPET: a dedicated mammary and axillary region PET imaging system for breast cancer, IEEE Trans. Nucl. Sci., Vol 48, (2001), pp 811 - 815



- [3] W. Enghardt, P. Crespo, F. Fiedler, R. Hinz, K. Parodi, J. Pawelke, F. Ponish, 2004 Charged hadron tumour therapy monitoring by means of PET, *Nucl. Instr. Meth. Phys. Res., A* 525 (2004), pp 284 - 288
- [4] M. Tsuchimochi, H. Sakahara, K. Hayama, M. Funaki, R. Ohno, T. Shirahata, T. Orskaug, G. Maehlum, K. Yoshioka, E. Nyard, A prototype small CdTe gamma camera for radioguided surgery and other imaging applications, *Eur. J. Nucl. Med. Mol. Imaging*, Vol 30, No 12 (2003), pp 1605 - 1614
- [5] L. Menard, Y. Charon, M. Solal, M. Ricard, P. Laniece, R. Mastrippolito, L. Pinot, L. Valentin, Performance characterization and first clinical evaluation of intra-operative compact gamma imager, *IEEE Trans. Nucl. Sci.*, Vol. 46, No 6, (1999), pp 2068 - 2074
- [6] N. Uzunov, M. Bello, P. Boccaccio, G. Moschini, G. Baldazzi, D. Bollini, F. de Notaristefani, U. Mazzi, M. Riondato, Performance measurements of a high-spatial-resolution YAP camera, *Phys. Med. Biol.*, 50 (2005), N11 – N21

#### 4) MEDICAL AND PHARMACOLOGICAL ACHIEVEMENTS OF THERAPEUTIC IMPACT

##### I. *In vivo* biodistribution scintigraphy imaging of a paclitaxel-hyaluronic acid bioconjugate

Position-sensitive gamma-ray detectors capable of imaging gamma emitters distributed in biological organisms represent sensitive and non-invasive instruments to perform *in vivo* studies of transport processes or metabolic trapping of radiopharmaceuticals as well as of molecular therapeutic agents. We employed the YAP camera to assess *in vivo* biodistribution of a new prototype derivative bioconjugate composed by paclitaxel linked to hyaluronic acid (paclitaxel-HA).. Biodistribution of the compound was studied following intravenous, intraperitoneal and intravesical administration.

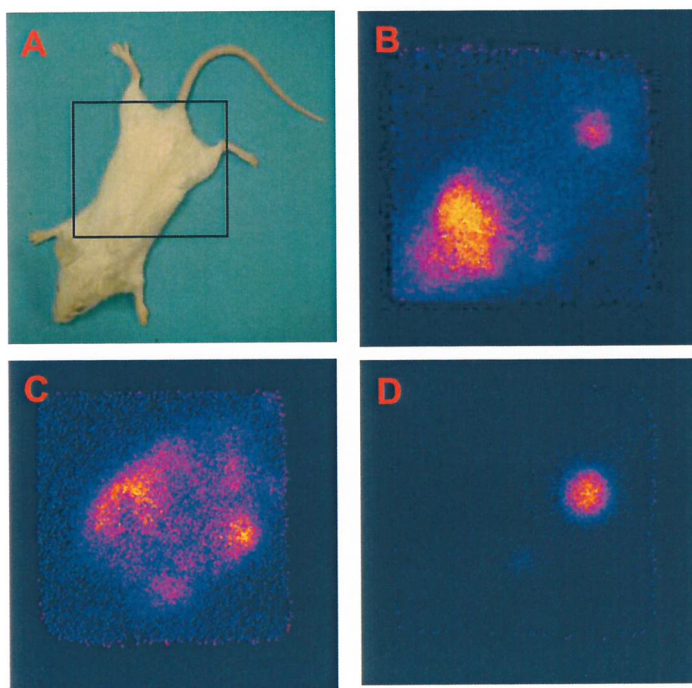


Figure 8. Biodistribution studies of paclitaxel-HA. *In vivo* distribution of  $^{99m}\text{Tc}$ -labeled bioconjugate was investigated in anesthetized mice (A) using a high-spatial resolution YAP gamma camera. Images reported were taken 2 hours after administration and refer to mice inoculated intravenously (B), intraperitoneally (C) or after bladder instillation (D).

After anesthetization, mice were inoculated with  $^{99m}\text{Tc}$ -labelled bioconjugate, and subsequently underwent imaging by the YAP camera for a 2 h period. Intravenous inoculation of the compound was followed by a strong liver uptake that reached 80% of the radioactive signal after 10 minutes and remained constant thereafter, thus indicating that this route of administration could be well suited to target primitive or metastatic liver neoplasias. Imaging of bladder and abdomen after regional administration disclosed that the radiolabeled bioconjugate remained confined to the cavities, suggesting a potential regional application for vesical and ovarian cancers. Therefore, preventive studies based on imaging analysis of new drugs may potentially dictate their therapeutic application *in vivo*.

## **II. Stability, biodistribution and dosimetry studies of $^{188}\text{Re}$ -hyaluronic acid, a potential radio therapeutic agent for hepatocarcinoma**

At the moment, the best results in cancer treatment have been obtained using the combined-modality therapy, meaning an antitumor agent radiolabelled with a beta emitter radionuclide. Recently a complex of the linear polysaccharide, hyaluronic acid, was labelled with  $^{99m}\text{Tc}$  by a direct method. Biodistribution studies showed that after 25 min of the intravenous administration more than 80 % of radiopharmaceutical was found in liver and spleen, attributable to both the lypophylic feature of the complex and the selective uptake of hyaluronic acid via receptors present in the liver and the spleen endothelial cells. Therefore the aim of this work was to assess the potential clinical use of HA labelled with  $^{188}\text{Re}$  for hepatocarcinoma therapy.  $^{188}\text{Re}$ -HA was obtained by incubation of  $\text{SnCl}_2$ ,  $^{188}\text{ReO}_4$  and HA for 90 min to 65 °C with a radiolabelling yield higher than 90%. HPLC and ITLC analysis showed that the complex was stable *in vitro* for more than 48 h. Pharmacokinetic studies in normal mice showed that 30 min after intravenous injection  $^{188}\text{Re}$ -HA was mainly localized in the liver and the spleen, and remained there for at less 72 h. The maximum tolerated radiation dose for the liver determined in normal mice was 309 Gy (obtained after injection of 37 MBq of  $^{188}\text{Re}$ -HA)..It was conclude the  $^{188}\text{Re}$ -HA showed enough stability and good pharmacokinetic characteristics to be used as radiotherapeutic agent for hepatocarcinoma.



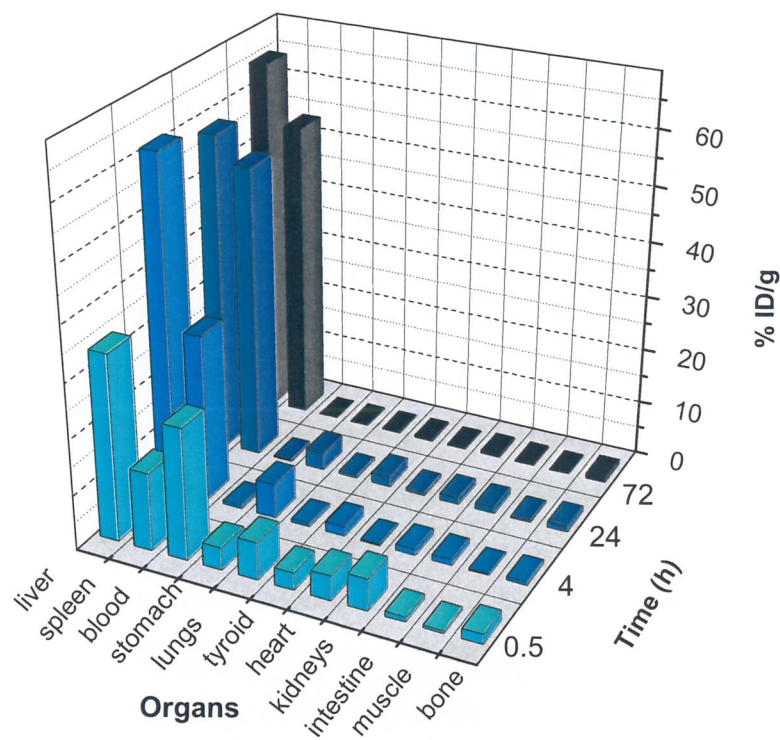


Figure 9. The weight-relative percentage of radioactivity detected in different organs and at different timepoints after i.v. administration of a single  $^{188}\text{Re}$ -HA dose.

### III. A novel radiotherapy approach based on $^{188}\text{Re}$ -hyaluronic acid for the liver-focused treatment of primary and metastatic tumors

Treatment of primary and metastatic liver tumors remains cumbersome. Previous work showed that  $^{99\text{m}}\text{Tc}$ -labelled hyaluronic acid (HA) undergoes a very rapid and selective uptake in liver following intravenous (i.v.) administration. Therefore, labelling of HA with the beta emitter  $^{188}\text{Re}$  congener might constitute a powerful tool to set up a liver-specific radiopharmaceutical to treat liver tumors. To assess this hypothesis, C57BL/6 mice were injected i.v. with M5076 tumor cells, a fibrosarcoma which peculiarly metastatizes at liver, and treated 7 days later with 9.2, 7.4, 4.5, and 2.2 Mbq of  $^{188}\text{Re}$ -HA. Two weeks later, mice

were sacrificed to evaluate the therapeutic impact. While livers of untreated mice exhibited a massive neoplastic infiltration and disclosed an enormous increment of weight, organs from treated animals were macroscopically normal.

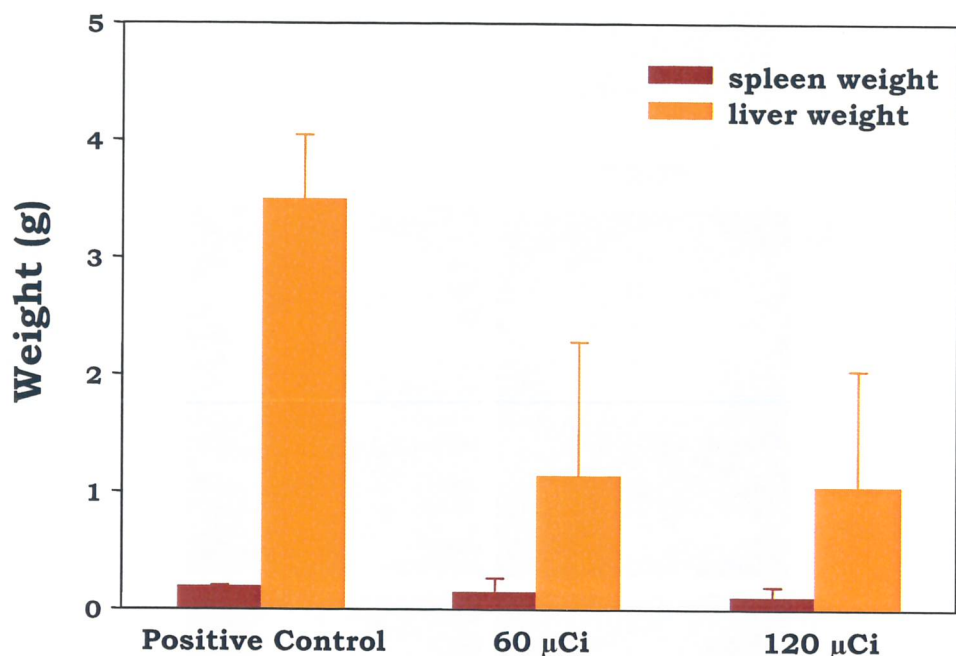


Figure 10. The weight (mean  $\pm$  SD) of spleen and liver from mice bearing M5076 tumor metastases and treated with 120  $\mu$ Ci or 60  $\mu$ Ci of  $^{188}\text{Re}$ -HA.

Few metastatic foci were only visible in livers of mice receiving the lowest activity. Similar results were also obtained in a xenogenic mouse model of human coloncarcinoma liver metastases employing HT-29 tumor cells implanted in SCID mice. Noteworthy,  $^{188}\text{Re}$ -HA treatment brought about a dramatic increase in survival in this mouse model. Overall,  $^{188}\text{Re}$ -HA radiotherapy approach was well tolerated and associated to mild liver and bone marrow toxicity. We are currently testing the therapeutic potentiality of multiple administrations of low activities of the radiopharmaceutical to afford a long-lasting curative effect, in order to set-up all experimental conditions for potential transfer to the clinical setting.

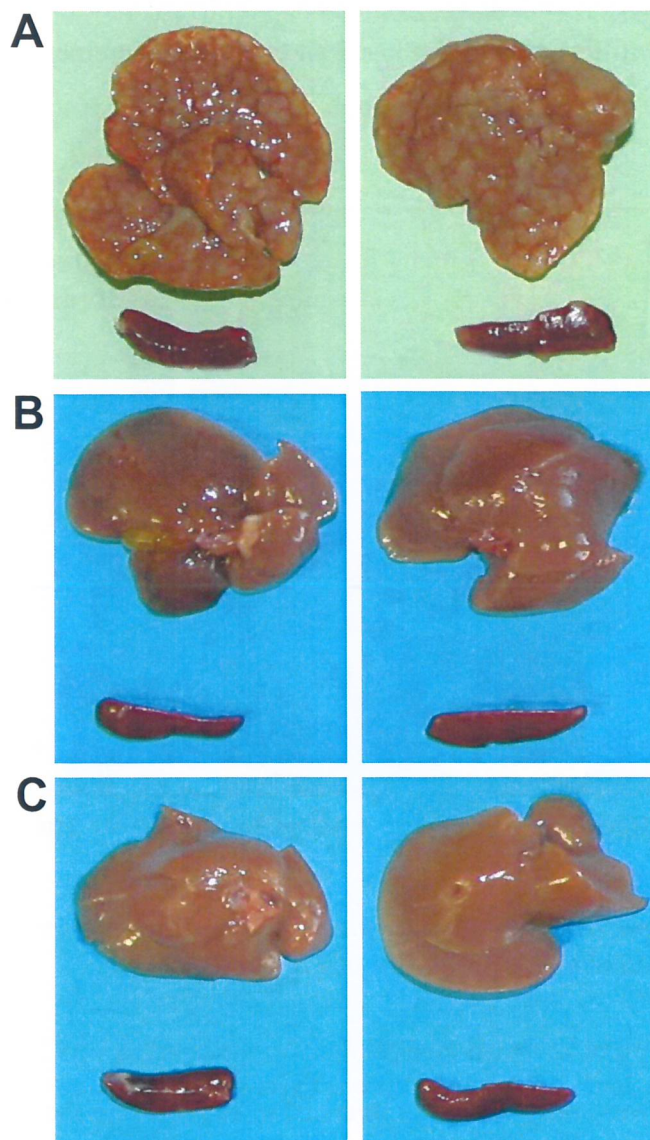


Figure 11. Pictures of livers and spleens explanted from mice injected with M5076 tumor cells at day 0 and treated at day +7 with saline (A), 60  $\mu\text{Ci}$  (B) or 120  $\mu\text{Ci}$  (C) of  $^{188}\text{Re}$ -HA. Animals were sacrificed at day 21 from tumor injection.

#### IV. Future Plans for tumor radiotargeting

Hybridoma technology makes available large quantity of mAb with high specificity towards various tumor-associated antigens. Although several radiolabeled mAbs are now commercially available as imaging agents of cancer and encouraging results have been



achieved in the treatment of hematopoietic malignancies, there remains a need for successfully treating solid tumors. One of the major problems is the low tumor-to-nontumor ratio of radioactivity accumulation due to the slow diffusion of the mAb into tumors and to their slow clearance from bloodstream. To solve these problems, pretargeting strategies have been investigated, multi-step approaches where the radionuclide is administered separately from the tumor-targeting mAb, thus allowing rapid and specific delivery of radioisotope to a tumour with minimal radiation exposure. Most of pretargeting studies employ the (strept)avidin-biotin system, for which different multistep injection schemes were developed: in the two-step method, (strept)avidin-conjugated mAb is administered first. In a later phase, when the mAb has accumulated in the tumor and the excess has cleared from the circulation, the radiolabeled biotin is injected and the radionuclide binds to the tumour cells thanks to the (strept)avidin-biotin interaction. In the three-step method the injection sequence starts with biotinylated mAb, followed by (strept)avidin (the "chaser", to remove the residual mAb from the bloodstream), and finally by radiolabelled biotin. We plan to use this latter approach to target prostate tumors with anti-PSMA mAb.

Survivin is a member of the inhibitor of apoptosis (IAP) gene family that is involved in the regulation of both cellular proliferation and apoptotic cell death. A crucial property of survivin is that it exhibits differential expression in nearly all human cancers while it is not expressed in most normal tissues. In this respect, survivin has been defined as an universal tumor antigen and represents the fourth most significant transcriptosome expressed in human tumors. Survivin overexpression in cancer compared to normal tissues makes it a potentially attractive target for cancer therapeutics, with a special emphasis to radiotherapeutics. To this aim, an emerging technology, LNA, could represent a terrific tool to develop an "universal" radiopharmaceutical. LNA represent a very innovative approach to antisense therapy and are constituted by a novel type of nucleic acid analogues that contain a 2'-O, 4'-C methylene bridge. This bridge restricts the flexibility of the ribofuranose ring and locks the structure into a rigid bicyclic formation, conferring exceptional biostability and enhanced hybridization performance towards complementary DNA and RNA. LNA are not easily recognized by nucleases, with a consequent increased lifetime both in vitro and in vivo, and they are also very stable over a wide pH range. The phosphate groups in the structural backbone facilitate their transportation into cell by utilizing traditional cationic vectors and confer good water-solubility to these compounds. Several experimental studies have shown the strong capacity of LNA to target and inhibit specific mRNA, both in vitro and in vivo. These characteristics

make LNA excellent candidates for the development of targeting strategies against tumor cells overexpressing specific mRNA.

Based on these premises, we plan to carry out the following tasks.

*Task 1. Assessment of in vitro tumor growth inhibition and radiobiological effects*

Following development of radiopharmaceuticals to be used in the research program, we will evaluate the capacity of  $^{188}\text{Re}$ -labelled therapeutic conjugates to inhibit tumor growth in vitro. To this end, human neoplastic cells of different histotypes (LnCaP prostate tumor cells, HT-29 colon cancer cells, positive for survivin expression, and MDA-MB-231 mammary tumor cells, that do not express survivin) will be seeded on 96 multi-well plates 24 hours before treatment, then exposed to different activities of radiopharmaceuticals, according to the different experimental models that are developed (LnCaP cells for  $^{188}\text{Re}$ -biotin and HT-29 and MDA-MB-231 cells for  $^{188}\text{Re}$ -LNA). The capability of radiation to affect tumour cells is evaluated with the MTT assay, which measures mitochondrial metabolism in the entire cell culture and is a recognized test for cytotoxicity and inhibition of cell proliferation. As an additional tool to monitor the radiosensitivity of treated cancer cells, the micronucleus (MN) test in the presence of the cytodieresis inhibitor Cytochalasin-B will be also carried out. Micronuclei are small nuclei which arise as result of clastogenic damage, leading to a loss of chromosome fragments at anaphase. As a consequence, the cytokinesis-blocked MN assay in BNC, when cells divide only once, is recognized as a measure of genotoxic damage. Finally, radio-induced apoptosis will be evaluated by means of three different approaches, that is scoring of apoptotic bodies, cells positive to the staining either to activated caspase-3 or TUNEL.

*Task 2. Tomography of radiopharmaceutical biodistribution in vivo*

Quantitative assessment of in vivo radiopharmaceutical biodistribution kinetics, after i.v. injection, will be carried out employing the tomography detector developed along the research program. These studies will be performed in immunodeficient SCID mice that are permissive to the growth of human xenogeneic tumor cells. In particular, we will analyze both normal and tumor-bearing mice. To assess  $^{188}\text{Re}$ -biotin biodistribution and selective accumulation at tumor site, LnCaP cells will be injected s.c.; similarly, SCID mice will be injected at day 0 with HT-29 tumor cells in one flank, and with MDA-MB-231 cells in the



opposite one. When tumors are palpable, mice will receive radiolabelled LNA and the differential accumulation of the radioactive tracer will be monitored by tomography.

*Task 3. Assessment of in vivo Maximal Tolerated Activity (MTA), organ toxicity and radiobiological effects*

Acute toxicity studies and MTA evaluation will be carried out in conventional and immunodeficient strains of mice. To this end, MTA will be defined as the maximal activity inducing a weight loss not exceeding 15% of mouse weight before injection. In vivo  $^{188}\text{Re}$ -biotin or  $^{188}\text{Re}$ -LNA administration could be associated with side-effects such as myelosuppression and in particular neutropenia. To verify this aspect, immunocompetent and SCID mice will be injected with radioactive compound at increasing activities. At different timepoints thereafter, blood samples will be collected and undergo leukocyte count and scattering cytometry analysis. To analyze irradiation-induced effects in vivo, radiobiological endpoints and apoptosis induction will be studied in tumours and in healthy tissues derived from animals treated with  $^{188}\text{Re}$ -conjugated biotin or LNA.

In particular, immunohistochemistry techniques on paraffin-embedded tissue sections will allow to determine induction of those genes involved in the response to DNA damage and apoptosis, using monoclonal antibodies against p53, CDKN1A and bax. Apoptosis induction will be assessed by means of the TUNEL assay which is a suitable and reliable method to detect DNA fragmentation also in paraffin-embedded sections. Molecular biology approaches based on quantitative Real time RT-PCR will provide relevant indications on the cellular pathways activated by the beta component of radiation emitted by  $^{188}\text{Re}$ .

*Task 4. Assessment of in vivo antitumor efficacy*

To evaluate the therapeutic efficacy, we will employ only  $^{188}\text{Re}$ -labelled radiopharmaceuticals. To this end, tumor-bearing SCID mice will be injected with increasing activities of radiopharmaceuticals, seven days after tumor induction. When tumors are implanted s.c., antitumor efficacy will be assessed by evaluating the reduction of scintigraphic signal due to tumor shrinkage and recording tumor growth curves in treated and control mice. Moreover, in all experimental models further experiments will allow to assess whether radiopharmaceuticals have a therapeutic impact and determine an increase in survival time in treated mice in comparison to control ones.



## II PART: WHO WE ARE

### DESCRIPTION OF TEAMS AND FACILITIES INVOLVED IN SCINTIRAD

- the Laboratory of Radioisotope and Radiopharmaceutical Studies (LRRS at LNL);
- the Veterinary Clinical Sciences Dep. and Hospital Clinics in Agripolis;
- the Bologna University and INFN team ;
- the Rome I University and INFN team;
- The Laboratory of Microelectronics – INFN Roma III (LMIC)
- the Nuclear Medicine Service of the IOV Radiotherapy Department, Padua

## LABORATORY OF RADIOISOTOPE AND RADIOPHARMACEUTICAL STUDIES (LRRS)

### Team

Giuliano Moschini, Alessandra Banzato, Michele Bello, Pasquale Boccaccio, Cecilia Giron, Ulderico Mazzi, Laura Melendez-Alafort, Anna Nadali, Antonio Rosato, Paolo Rossi, Nikolay Uzunov, Elena Zangoni

### Activity and facilities

The LRRS at the National Laboratories of Legnaro, INFN is dedicated to explore new radiopharmaceuticals for the imaging diagnostics and radiotherapy as well as to develop new detecting systems and instrumentation to control and visualize the radio-traced tissues and organs.



Figure 1. *Laboratory for radio-chemical analysis. The cell for radio-isotopes manipulation*

The radio-chemical laboratory (Fig. 1 and Fig. 2) is a part of LRRS and is authorized to use radio-nuclides, such as  $^{99m}\text{Tc}$ ,  $^{18}\text{F}$ ,  $^{68}\text{Ga}$ ,  $^{188}\text{Re}$ ,  $^{64}\text{Cu}$ ,  $^{178}\text{Ta}$  for both synthesis and quality control of injectable radiotracers. The laboratory has facilities and structures for fully preparing samples of  $^{99m}\text{Tc}$  and  $^{188}\text{Re}$  ready to be injected in small animals for bio-distribution studies.

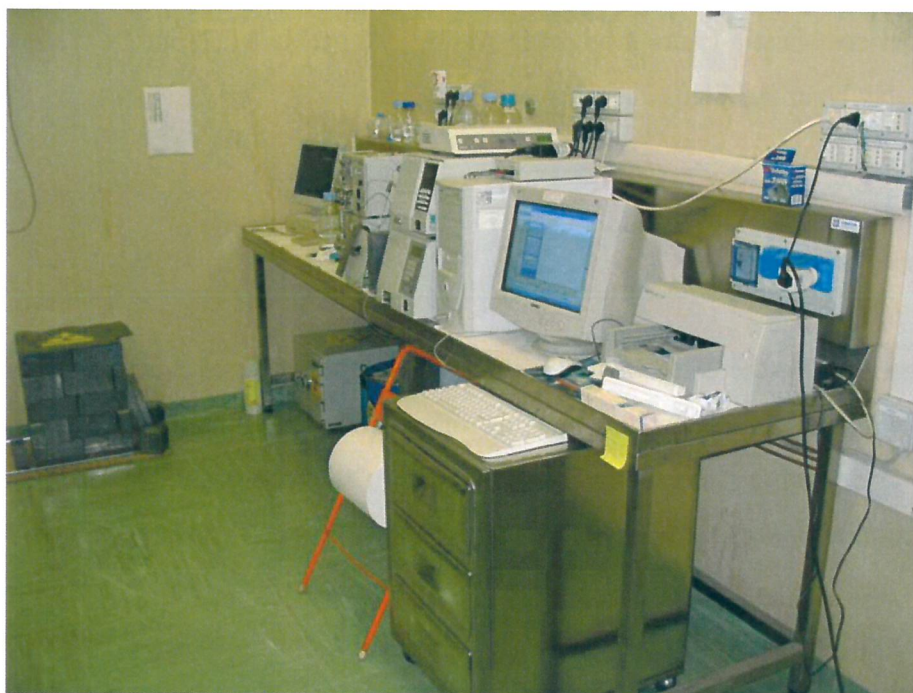


Figure 2. *Laboratory for radio-chemical analysis. System HPLC*

The synthesis and characterization of  $^{99m}\text{Tc}$  and  $^{188}\text{Re}$ -labeled compounds are carried out in collaboration with the Department of Pharmaceutical Sciences, featuring a multi-years experience in the field. The *in vivo* tests on small animals are done in collaboration with the Veterinary Clinical Sciences Department (Agripolis).

The usual procedure foresees a chemical evaluation of several Technetium-99 and natural Rhenium coordination complexes and their physico-chemical characterization employing tools such as: UV-visible and IR spectrophotometers; NMR, Mass Spectrometers; and X-ray diffractometers. This complete characterization is necessary since the new radio-labeled compounds, actually present in the injecting vial, can be defined only indirectly, by comparing (through a High Performance Liquid Chromatography HPLC) their chromatographic behavior to the one of already known compounds (completely characterized



by their physical-chemical data). A second step is the search for a labeling procedure that gives the highest production yields of a single compound having high specific activity.

The projects related to the radiotherapy application of  $^{188}\text{Re}$ -labelled radiopharmaceuticals follow the same steps, being always dedicated to the production of radio-labeled compounds to be injected *in vivo*. In this case, is carried out also a dosimetric evaluation to assess the amount of activity needed for the highest therapeutic effectiveness.

Two fully equipped systems for small-object gamma-ray imaging give the possibility to conduct *in vivo* biodistribution experiments with small animals. The systems are based on high-spatial resolution position-sensitive scintillator cameras employing segmented YAP scintillators.

One of the gamma-ray imaging systems is designed to operate with  $^{99\text{m}}\text{Tc}$ -labelled radiopharmaceuticals (Figure 3). It has a parallel-hole collimator to ensure parallel entrance of the gamma rays. The holes have diameter of 0.5mm and are situated at a relative distance of 0.65mm from one another. The field of view (FOV) of the gamma camera (i.e. the maximum imaging area) with this collimator is 40 x 40 mm. The geometry of the collimator ensures a very good spatial resolution which is less than 1.5mm for the most used distances to the imaged objects.



Figure 3. Laboratory for radio-chemical analysis. System for imaging using  $^{99\text{m}}\text{Tc}$

As an illustration of the YAP camera performance, in figure 4 we present some images acquired from a mouse, treated with  $^{99m}\text{Tc}$  labeled Hyaluronic acid (HA). The labeling is done applying a direct method. HA is a linear glycosaminoglycane constituted by repeating D-glucuronic acid and N-acetyl-D-glucosamine dimers. It has been chosen because its biodistribution pathways are very simple and its uptake is up to 80% of injected activity located into the liver. The 250  $\mu\text{l}$  of  $^{99m}\text{Tc}$ -HA (27.27 MBq) in 3 mg/ml have been administrated to a healthy male mouse (C57/Bl) via tail vein, after anesthesia with Lavertin. The images show the activity of the abdominal part of the mouse taken for time intervals of five minutes. Regions of interest (ROI) corresponding to the position of the liver and urine bladder are shown on the images.

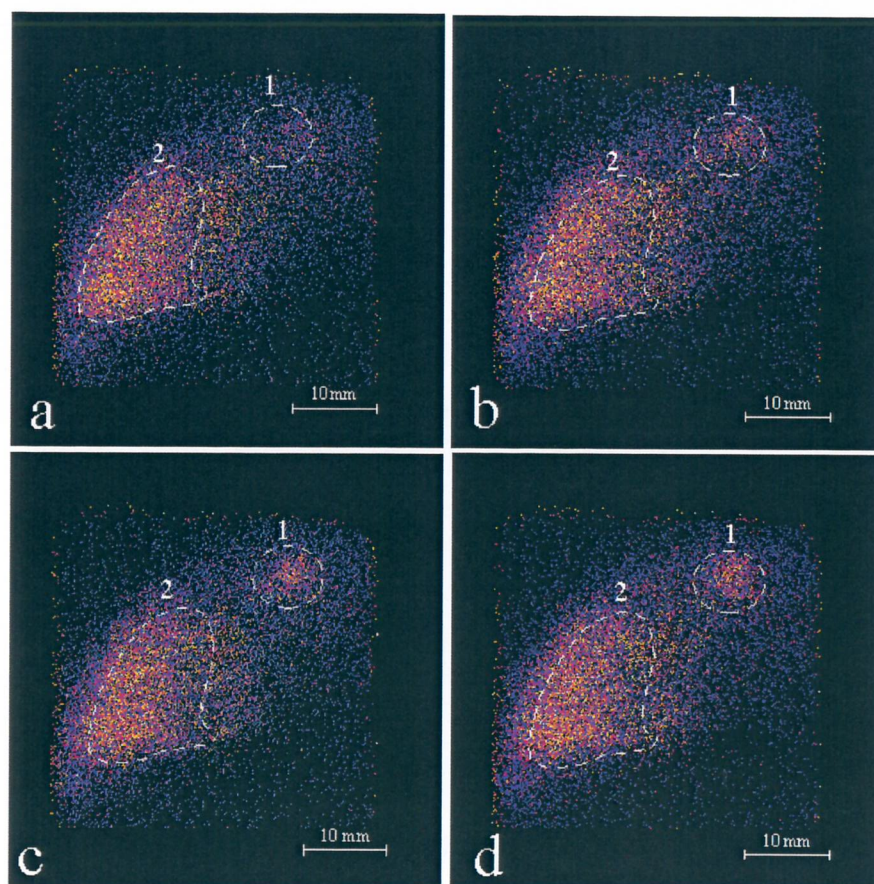


Figure 4. *In vivo* images of activity of mouse body regions comprising sovradiafragmatic and subdiafragmatic organs, treated with  $^{99m}\text{Tc}$ -HA. The images are made at four consequent acquisition times after the injection: image **a** for time interval 0-5min; image **b** for 5-10min; image **c** for 10-15min and image **d** for 15-20min. With 1 is indicated the position of the mouse bladder and with 2 – the position of the liver.



The other imaging system is designed to operate with  $^{188}\text{Re}$ -labelled radiopharmaceuticals. Such radiopharmaceuticals have some advantages compared to the widely used  $^{99\text{m}}\text{Tc}$  for small animal imaging. However, some specific aspects have to be considered when  $^{188}\text{Re}$  is employed for imaging purpose.  $^{188}\text{Re}$  isotope decays to  $^{188}\text{Os}$  via  $\beta$ -particle emission with an energy distribution extending up to 2.12 MeV. The isotope  $^{188}\text{Os}$  itself emits almost promptly a 155 keV gamma-ray which is used for the imaging with position-sensitive detectors. However,  $^{188}\text{Os}$  emits also beta-rays with energies up to 2 MeV. The different emission properties of  $^{188}\text{Re}$  (compared to  $^{99\text{m}}\text{Tc}$ ) imply a different design of the imaging cameras in order to reduce both the  $\beta$ -ray interference and the higher image background due to higher-energies gamma-rays. In this respect, a high-spatial-resolution position-sensitive camera for imaging of small animals treated with this isotope has been designed and assembled at the LRRS (Figure 5).



Figure 5. *Imaging room. High-spatial resolution camera for imaging using  $^{188}\text{Re}$*

The  $^{188}\text{Re}$ - imaging camera has a field of view 50mm x 50mm and a spatial resolution of 2.7mm at an object-to-camera distance 10mm.

Work on a tomographic system based on two position-sensitive photomultiplier tubes type H8500 and exploiting  $\text{LaBr}_3:\text{Ce}$  scintillator is in progress. The main part of the



experimental set-up of the tomographic system is compounded by two mutually perpendicular situated position-sensitive photomultiplier tubes (PSPMT) Hamamatsu H8500. The sensitive surface of this device has dimensions of  $52 \times 52 \text{ mm}^2$  and the system could be used for small animal SPECT. The system is to be accomplished at the end of October 2006.

A method to measure the detector-to-object distance from the images obtained with a stationary high-spatial-resolution gamma-ray camera for in-vivo small-object studies has been developed in the LRRS. It exploits the shift of the imaged object in the image plane, obtained for tilted positions of a parallel-hole collimator (patent No RM 2006 A 000216, UIBM Roma). In this way three-dimensional information about the object position can be obtained without moving either the camera or the object. The effectiveness of the method has already been tested for point-like gamma-ray emitting objects as well as for some three-dimensional small-size objects. Gamma-ray images from spherically shaped cavities filled with a solution of  $^{99\text{m}}\text{Tc}$  at different depth position in tissue equivalent phantoms have been analyzed. A linear dependence of the image displacement on the distance to the object has been measured using a modified tilted-collimator scintillation YAP camera. Similar behavior has been shown for some asymmetric small-size cavities. A work on a prototype of an instrument utilizing the developed method and equipped with a computer-guided manipulator is in progress. The manipulator has three degrees of freedom and is designed for on-line operations such as e.g. needle biopsy.

**THE VETERINARY CLINICAL SCIENCES DEPARTMENT AND HOSPITAL:  
INTERNAL MEDICINE OF SMALL AND LARGE ANIMALS  
(Agripolis, Legnaro-Padova)**

**People**

D. Bernardini, G. Gerardi, A. Zotti, A. Giuliani, M. Coppola, S. Testoni, H. Poser, students and postdocs.

**Activities**

The Department is committed to clinical activities (medical, obstetric and surgical), teaching duties at various levels and a forefront research agenda.

The Hospital's many wards of internal and surgical medicine cover the whole range of animal care and feature advanced equipment. The Hospital offers a widespread regional service and is a template for similar structures in the area. It also forms the base of an effective teaching. We teach many subjects at under-graduated and graduated level as part of the Degrees curricula of the Faculty of Veterinary Medicine. We also hold advanced classes on specialized subjects for doctors and practitioners members of professional affiliations. Broad and Intense is the seminar and tutorial practice.

We pursue a wide range of research projects, regarding matters such as:

- pathologies of "non-conventional" animals, like snakes, turtles, ...;
- genetic etiology of the new disorders in domestic animals;
- study of blood concentration of some enzymes and hormones;
- new surgical and reproductive techniques;
- boosting the imaging diagnostics by employing new Nuclear Medicine methods and apparatus.

## Facilities

1) Hematology, Urology and Clinical Biochemistry Laboratory. It employs several up to dated apparatus, such as:

-A full blood count analyzer, model ADVIA-120 (Bayer), able to automatically handle different species, like dogs, cats, bovine, horses, rodents (mice and rats), rabbits, and monkeys (Figure. 1)

-A serum clinical chemical analyzer, model IMULITE-1000 (DPC, USA). It is mainly used for hormonal dosage in allergic and reproductive disorders and for detection of tumor markers.

- A Mass Chromatographer and Spectrometer again for serum analysis. It is calibration free as its outcomes do not depend upon the matrix composition. It is mainly employed for the non conventional animals (snakes, turtles, etc.) serum analysis.

- A HPLC (High Performance Liquid Chromatographer).

2) The Veterinary Hospital, including several branches, such as:

-veterinary's offices for the medical examinations

-rooms for diagnostics imaging equipment, like X-ray equipment for film recording, X-ray fluoroscopy with image intensifier for dynamic inspection, Ultrasound, Endoscopy, Arthroscopy, Bones Densitometry, TAC and Anger Camera for Scintigraphy (Figures 2 ,3, 4).



Figure 1. *ADVIA-120 (Bayer)*



Figure 2. *X-ray with film recording.*



- 3) The Recovery Ward, including horses and bovine boxes and external paddocks (Figure 6)
- 4) The Teaching Division
- 5) The Surgical Ward (Figure 5)
- 6) The Experimentation Animals' Ward with a stabularium inclusive of rodents, sheep, swine, dogs, etc.



Figure 3. *TAC for small animals.*



Figure 5. *Surgery Room for small animals.*

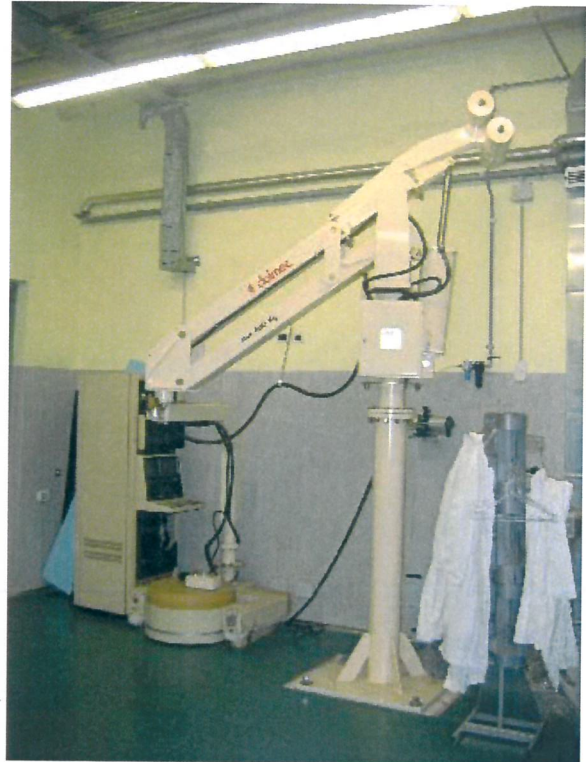


Figure 4. *Anger Camera for large animals.*



Figure 6. *Air conditioned Horse stable.*

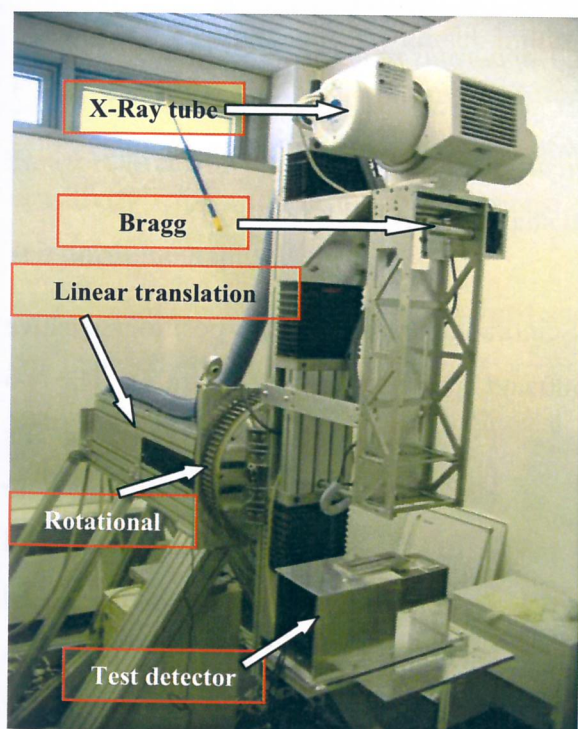
## THE BOLOGNA UNIVERSITY AND INFN TEAM

### People

D. Bollini, F.L. Navarria, G. Baldazzi, A. Perrotta, Mirko Zuffa

### Activity and facilities

The group is dedicated to the study and development of innovative medical instrumentation and detectors in the fields of X-rays and  $\gamma$ -rays. The laboratory for electronic design and instrumentation test, in association with the electronics and mechanics laboratories of the INFN of Bologna are our main resource.



Regarding X-rays, we are developing a new multi-energy TC to study the tumor development and metastasis formation in small animals and identify election applications of the innovative multi-energy technique (Figure 1).

Figure 1. *The multi-energy TC apparatus.*

Our study of  $\gamma$ -Rays led to the first microSPECT developed during this work (shown in Figure 2). With this facility we have performed an extensive set of measurements regarding the  $^{188}\text{Re}$  transport properties with an innovative technique. A further study on the tissue issued dose, through imaging, was also performed.



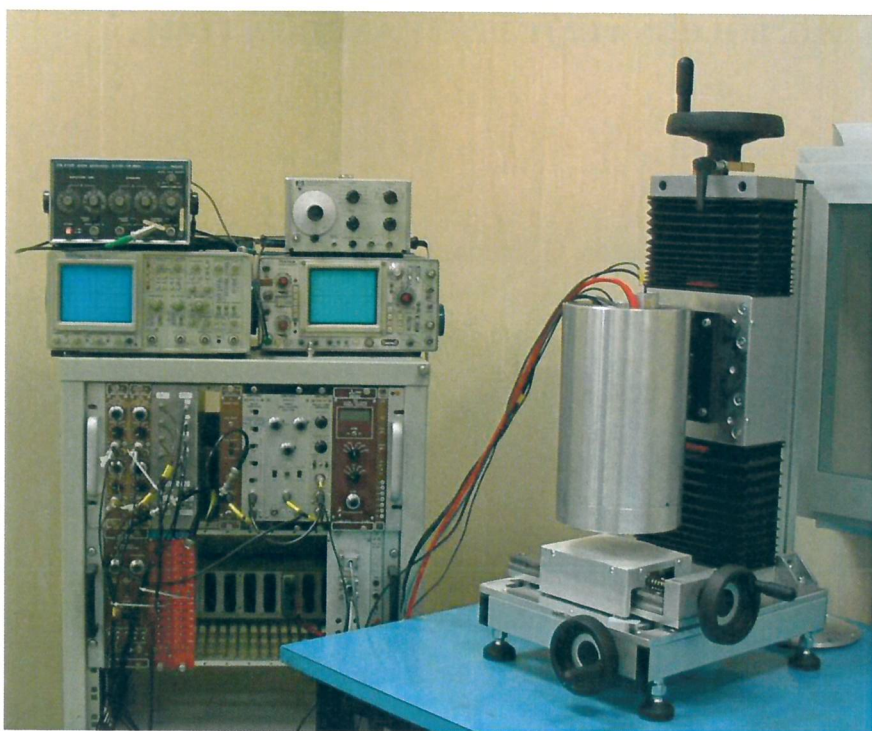
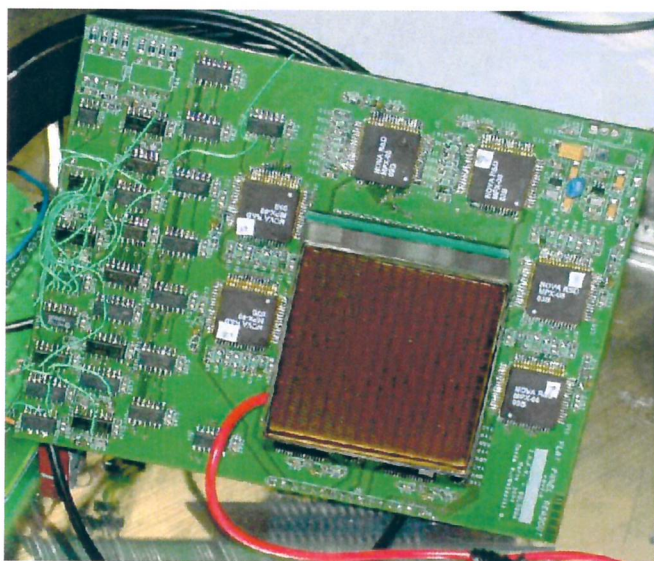


Figure 2. *The first SPECT apparatus realized.*

This microSPECT is now working at *Technological Pole* of the *S. Orsola University Hospital* in Bologna where a centre for animal pre-clinical study is working.

The new microSPECT developed for Scintirad is based on two position-sensitive photomultiplier tube (PSPMT) Hamamatsu H8500 and is now under test (Figure 3). The two



PSPMTs – each one fitted on its electronic board – are coupled to LaBr<sub>3</sub>:Ce scintillator slabs and lead collimators, and housed inside a lead shield. The instrument features two orthogonal measurements heads that can rotate around the mouse.

Figure 3. *The H8500 and R/O electronics.*



## THE ROME I AND INFN TEAM AND FACILITY

### People

R.Pani, M.Mattioli, R.Pellegrini, R.Scaf , M.N.Cinti, P. Bennati, M.Betti, V.Casali

### Activity and facilities

We are committed to explore and design new gamma ray detectors, based on scintillation crystals, for medical imaging. Over the last 15 years we have been developing different gamma cameras and probe imagers for human and small animal applications.

In 1993 the team has developed (INFN, Hirespet collaboration) a novel small field of view (FoV) gamma camera with sub-millimeter spatial resolution for small animal imaging (YAP Camera). In 1995 we invented for INFN a novel gamma camera dedicated to scintimammography (SPEM), showing how a good positioning can enhance the clinical sensitivity for sub-centimeter lesions, 60% more than obtained by standard scintimammography.

Subsequently, the group designed and built a more advanced gamma camera (20x15 cm<sup>2</sup>) based on a small PSPMT array capable of a large FoV, dedicated to scintimammography (INFN technological transfer, founded by the Italian government, L.46/art.10). In collaboration with the Department of Nuclear Medicine of the Umberto I Hospital (University of Rome "La Sapienza"), we have tested this gamma camera employing radiopharmaceuticals, typically used in clinical trials, and in vivo experiments.

The latest innovation introduced by the group in term of clinical trials for scintimammography is a dual heads detector to obtain co-registered image of a breast in cranio-caudal projection as in figure 1 (funded by "IMI" Italian project for the INFN technological transfer). A first head consists of the multi PSPMT camera; the second head is a probe, 2 inch square, based on planar LaBr<sub>3</sub>:Ce, 50.8x50.8 mm<sup>2</sup> size and 10 mm thick with a 3 mm thick glass window, coupled to Hamamatsu H8500 Flat Panel PMT . In the near future the group is going to test the first laBr<sub>3</sub>:Ce gamma camera with 10 x10 cm<sup>2</sup> FoV.

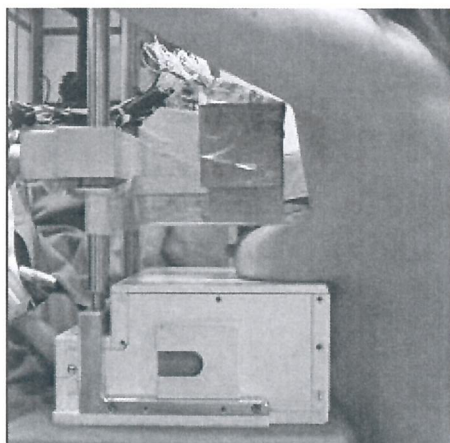


Figure 1. *A dual heads detector to obtain co-registered image of a breast in cranio-caudal projection.*

The group has a number of important collaborations with international research centers, in particular with Johns Hopkins Maryland–USA and Jefferson Lab, Virginia-USA.

## LABORATORY OF MICROELECTRONICS – INFN ROMA TRE (LMIC)

### Team

Francesco de Notaristefani, Valentino Orsolini Cencelli, Enrico D'Abramo, Andrea Fabbri, Francesco Petullà, Domenico Riondino.

### Activity and Facilities

The LMIC at the INFN, Section “Roma Tre”, is dedicated to the development of electronic and microelectronic circuits for application in Medical Imaging. The laboratory is specialized in ASIC full custom design using the most recent deep submicron technologies. The LMIC is equipped with a full featured CAD environment including electronic design software supplied by world leading producers like Cadence, Synopsys, Mentor Graphics and Altera. The CAD runs on both Intel based workstations (Linux OS), and Sun Sparc (Solaris OS). A tool for symbolic circuit analysis, based on Mathematica, is also used in early phases of design.

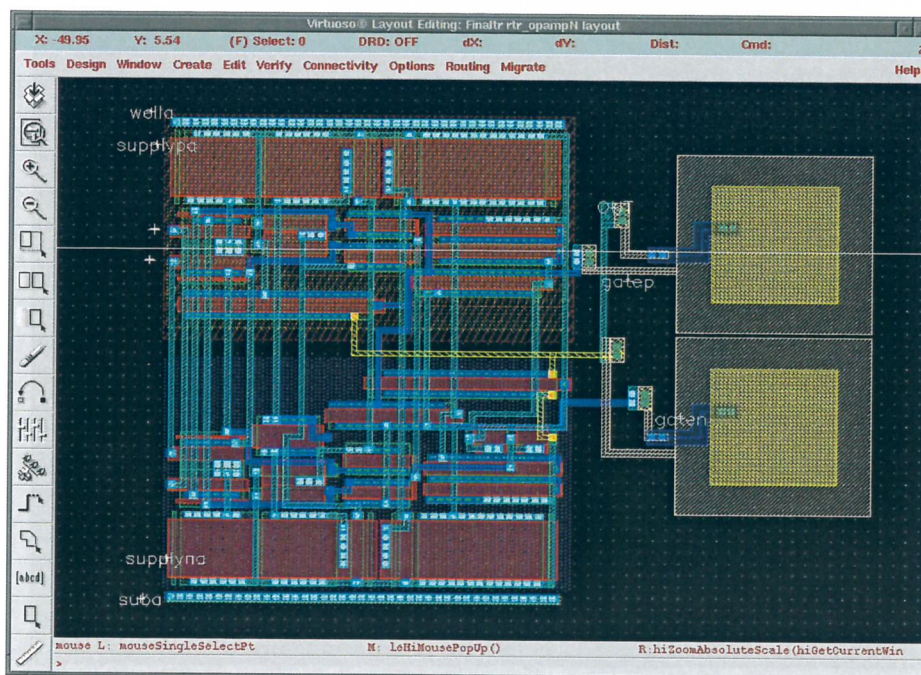


Figure 1. Layout of a rail-to-rail operational amplifier in UMC 0.25u technology.



The LMIC has also the know-how to design and test standard PCBs based on commercially available integrated circuits and discrete components, and has also developed the capability of complex FPGA and microcontroller based systems. The lab performs all the operations in the IC design-production-test cycle, including the in-house wire-bonding (Figure 2), and has developed many IC test boards (in Figure 3 a test board based on the Altera ACEX 1K).



Figure 2. *Hybond manual bonding machine*

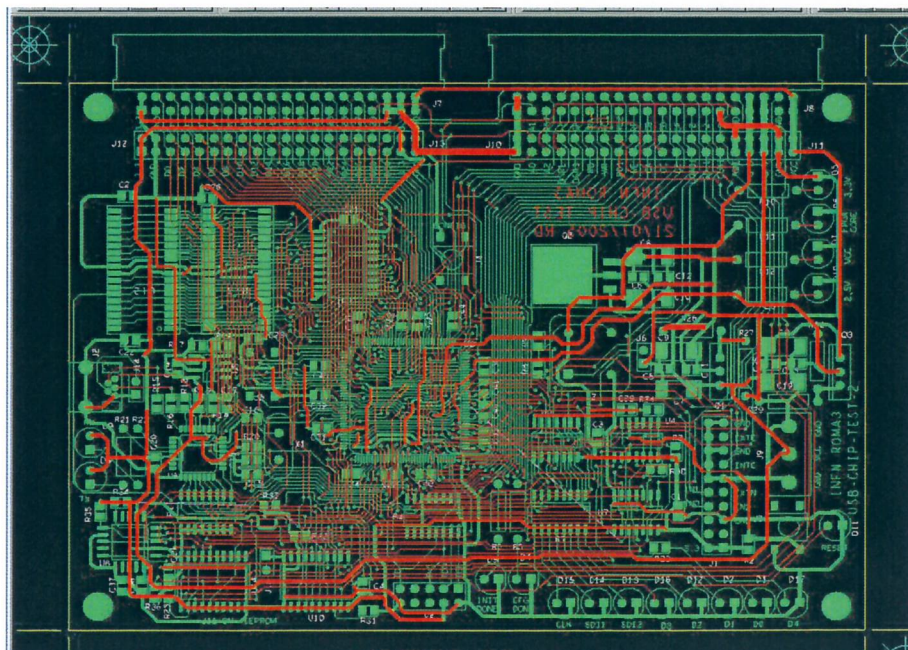


Figure 3. *A test board layout*

Since its foundation in 1999, the lab has produced several chips dedicated to near infrared (i.e. Figure 4) and gamma imaging.

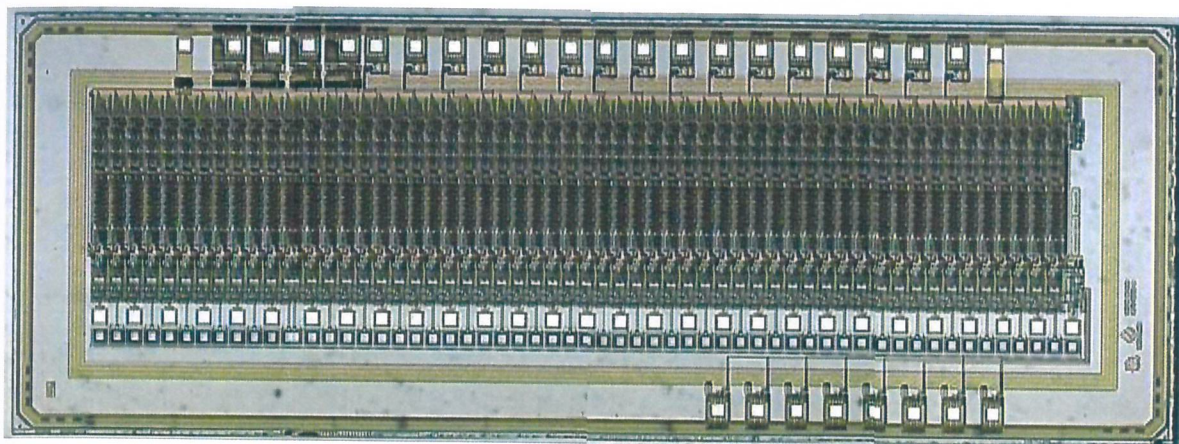


Figure 4. *The NIRCAM, a near infrared camera prototype.*

Today the LMIC is producing a new readout for the flat panel, multi anode, position sensitive PMT Hamamatsu H8500. The system reads in parallel the PMT 64 anodes and can be connected to a PC through a USB port. We are also designing an application specific IC to read the H8500 with a single chip. This ASIC will be used to build a wide FOV gamma camera (10cm x 10cm) based on a single LaBr3 crystal coupled with four H8500. Please, note also in Figure 1 a Cadence Virtuoso screen shot showing a CMOS 0.25u rail-to-rail operational amplifier to be used in the Charge Sensitive Amplifier of the new ASIC.



# **ISTITUTO ONCOLOGICO VENETO**

## **Operative Unit of Radiotherapy**

**(Director Guido Sotti, MD)**

## **Service of Nuclear Medicine**

**(Responsible Dario Casara, MD)**

### **Medical Team**

Dario Casara (MD), Giorgio Saladini (MD), Annarita Cervino (MD), Salvatore Santarcangelo (researcher)

### **Technical Team**

Giancarlo Zonzin (coordinator), Laura Memo, Elena Zaramella, Marino Bortolami, Giorgio Masiero, Riccardo Sanco

### **Activities**

Nuclear Medicine Service is a diagnostic division of Radiotherapy Department of Istituto Oncologico Veneto (IOV), chairman of the Department is dott. Guido Sotti. The NM Service is dedicated to diagnosis and disease staging of patients affected by cancer. We use different radiopharmaceuticals labeled by  $^{99m}\text{Tc}$ ,  $^{111}\text{In}$ ,  $^{131}\text{I}$  or other radio-nuclides, both for detection of tumor sites or for general purpose studies such as cardiac, renal or respiratory function assay.

Clinical and functional images are obtained using single or dual head gamma cameras assisted by a computer with advanced clinical software. In these last weeks a new instrument was acquired by the Nuclear Medicine Service and physical and pre-clinical test are running: a Positron Emission Tomograph coupled with a 16 slices CT.



During last year more than 11,000 imaging tests were performed by this Nuclear Medicine Service on 7,000 cancer patients: in particular 2,900 whole body (WB) bone scans, 750 WB with <sup>131</sup>I for thyroid cancer, 800 lymphoscintigraphies for sentinel node detection in patients with breast cancer or cutaneous melanoma, 750 myocardium perfusion scans, 600 WB FDG PET-CT, 500 thyroid scans, 150 parathyroid scans, 150 WB scans with <sup>111</sup>In octreotide etc.

### Recent Papers

TONIATO A, CASARA D, PELIZZO M. The Negative Sestamibi Scan: Is a Minimally Invasive Parathyroidectomy Still Possible?. *Ann Surg Oncol.*, 2007 Nov 7, [Epub ahead of print] No abstract available. PMID: 17987345 [PubMed - as supplied by publisher]

PELIZZO MR, MERANTE BOSCHIN I, TONIATO A, PIOTTO A, BERNANTE P, PAGETTA C, CASALIDE E, MAZZAROTTO R, CASARA D, RUBELLO D. Papillary thyroid microcarcinoma. Long-term outcome in 587 cases compared with published data, *Minerva Chir*, 2007 Oct, 62(5)315-25. Italian. PMID: 17947943 [PubMed - in process]

MIAN C, BAROLLO S, PENNELLI G, PAVAN N, RUGGE M, PELIZZO MR, MAZZAROTTO R, CASARA D, NACAMULLI D, MANTERO F, OPOCHER G, BUSNARDO B, GIRELLI ME. Molecular characteristics in papillary thyroid cancers (PTCs) with no (<sup>131</sup>I) uptake. *Clin Endocrinol (Oxf)*, 2008 Jan, 68(1)108-16. Epub 2007 Sep 14. PMID: 17854396 [PubMed - in process]

RUBELLO D, SALVATORI M, CASARA D, PIOTTO A, TONIATO A, GROSS MD, ALNAHHAS A, MUZZIO PC, PELIZZO MR. <sup>99m</sup>Tc-sestamibi radio-guided surgery of loco-regional <sup>131</sup>Iodine-negative recurrent thyroid cancer. *Eur J Surg Oncol.*, 2007 Sep, 33(7)902-6. Epub 2007 Jan 30. PMID: 17267163 [PubMed - indexed for MEDLINE]

PELIZZO MR, RUBELLO D, BOSCHIN IM, PIOTTO A, PAGETTA C, TONIATO A, DE SALVO GL, GIULIANO A, MARIANI G, CASARA D. Contribution of SLN investigation with <sup>99m</sup>Tc-nanocolloid in clinical staging of thyroid cancer: technical

feasibility. *Eur J Nucl Med Mol Imaging*, 2007 Jun, 34(6)934-8. Epub 2007 Jan 18. PMID: 17235530 [PubMed - indexed for MEDLINE]

RUBELLO D, PELIZZO MR, CASARA D, PIOTTO A, TONIATO A, FIG L, GROSS M. Radio-guided surgery for non-131I-avid thyroid cancer. *Thyroid*, 2006 Nov, 16(11)1105-11. PMID: 17123337 [PubMed - indexed for MEDLINE]

MOCELLIN S, PILATI P, DA PIAN P, FORLIN M, CORAZZINA S, ROSSI CR, INNOCENTE F, ORI C, CASARA D, UJKA F, NITTI D, LISE M. Correlation between melphalan pharmacokinetics and hepatic toxicity following hyperthermic isolated liver perfusion for unresectable metastatic disease. *Ann Surg Oncol*. 2007 Feb, 14(2)802-9. Epub 2006 Nov 14. PMID: 17103263 [PubMed - indexed for MEDLINE]

PELIZZO MR, MERANTE BOSCHIN I, TONIATO A, PIOTTO A, BERNANTE P, PAGGETTA C, DE SALVO GL, CARPI A, RUBELLO D, CASARA D. Sentinel node mapping and biopsy in thyroid cancer: a surgical perspective. *Biomed Pharmacother*, 2006 Sep, 60(8)405-8. Epub 2006 Sep 1. PMID: 16962736 [PubMed - indexed for MEDLINE]

RUBELLO D, FIG LM, CASARA D, PIOTTO A, BONI G, PELIZZO MR, SHAPIRO B, SANDRUCCI S, GROSS MD, MARIANI G, ITALIAN STUDY GROUP ON RADIO-GUIDED SURGERY AND IMMUNOSCINTIGRAPHY (GISCRIS). Radioguided surgery of parathyroid adenomas and recurrent thyroid cancer using the "low sestamibi dose" protocol. *Cancer Biother Radiopharm.*, 2006 Jun, 21(3)194-205. PMID:16918295 [PubMed - indexed for MEDLINE]

IORE D, BAGGIO V, RUOL A, BOCUS P, CASARA D, CORTI L, MUZZIO PC. Multimodal imaging of esophagus and cardia cancer before and after treatment, *Radiol Med (Torino)*, 2006 Sep, 111(6)804-17. Epub 2006 Aug 11. English, Italian. PMID:16896560 [PubMed - indexed for MEDLINE]

RUBELLO D, PELIZZO MR, AL-NAHHAS A, SALVATORI M, O'DOHERTY MJ, GIULIANO AE, GROSS MD, FANTI S, SANDRUCCI S, CASARA D, MARIANI G. The role of sentinel lymph node biopsy in patients with differentiated thyroid carcinoma.



*Eur J Surg Oncol.*, 2006 Nov, 32(9)917-21. Epub 2006 Apr 18. Review. PMID:16621423  
[PubMed - indexed for MEDLINE]

ROSSI CR, DE SALVO GL, TRIFIRÒ G, MOCELLIN S, LANDI G, MACRIPÒ G, CARCOFORO P, RICOTTI G, GIUDICE G, PICCIOTTO F, DONNER D, DI FILIPPO F, MONTESCO MC, CASARA D, SCHIAVON M, FOLETTTO M, BALDINI F, TESTORI A. The impact of lymphoscintigraphy technique on the outcome of sentinel node biopsy in 1,313 patients with cutaneous melanoma: an Italian Multicentric Study (SOLISM-IMI). *J Nucl Med.* 2006 Feb, 47(2)234-41. PMID:16455628 [PubMed - indexed for MEDLINE]

RUBELLO D, VITALIANI R, RIGONI MT, RAMPIN L, GIOMETTO B, CASARA D, ZONZIN GC, ZAVAGNO G, CAPIRCI C, SHAPIRO B, MUZZIO PC. A rare case of paraneoplastic cerebellar degeneration discovered by whole-body F-18 FDG PET, *Clin Nucl Med.* 2005 Oct, 30(10)704-6. PMID:16166852 [PubMed - indexed for MEDLINE]

ZAVAGNO G, RUBELLO D, FRANCHINI Z, MEGGIOLARO F, BALLARIN A, CASARA D, DENETTO V, MARCHET A, RAMPIN L, POLICO C, NITTI D, MARIANI G; ITALIAN STUDY GROUP ON RADIOGUIDED SURGERY AND IMMUNOSCINTIGRAPHY. Axillary sentinel lymph nodes in breast cancer: a single lymphatic pathway drains the entire mammary gland, *Eur J Surg Oncol.* 2005 Jun, 31(5)479-84. Epub 2005 Apr 26. Erratum in: *Eur J Surg Oncol.* 2006 Feb, 32(1)e1. PMID:15922882 [PubMed - indexed for MEDLINE]

MIOTTO D, MIOTTO D, BERTOLO S, MINANTE M, DARISI T, MOCELLIN S, CASARA D, ORI C, FOLETTTO M, ROSSI CR, LISE M, NITTI D. Hypoxic antiblastic stop-flow perfusion: clinical outcome and pharmacokinetic findings, *J Chemother.* 2004 Nov, 16 (Suppl 5)44-7. PMID: 15675477 [PubMed - indexed for MEDLINE]

LISE M, PILATI P, DA PIAN P, MOCELLIN S, ORI C, CASARA D, ROSSI CR, DARISI T, CORAZZINA S, NITTI D. Hyperthermic isolated liver perfusion for unresectable liver cancers: pilot study. *J Chemother.* 2004 Nov, 16 (Suppl 5)37-9. PMID: 15675475 [PubMed - indexed for MEDLINE]



RUBELLO D, ZAVAGNO G, BOZZA F, LISE M, DE SALVO GL, SALADINI G, MARIANI G, CASARA D. Analysis of technical and clinical variables affecting sentinel node localization in patients with breast cancer after a single intradermal injection of 99mTc nanocolloidal albumin. *Nucl Med Commun.* 2004 Nov, 25(11)1119-24. PMID: 15577591 [PubMed - indexed for MEDLINE]

PILATI P, MOCELLIN S, MIOTTO D, FITTÀ C, CASARA D, ORI C, SCALERTA R, NITTI D, LISE M, ROSSI CR. Hypoxic antiblastic stop-flow limb perfusion: clinical outcome and pharmacokinetic findings of a novel treatment for in transit melanoma metastases. *Oncol Rep.*, 2004 Oct, 12(4)895-901. PMID: 15375519 [PubMed - indexed for MEDLINE]

RUBELLO D, PAGETTA C, PIOTTO A, CASARA D, ZONZIN GC, MUZZIO PC, PELIZZO MR. Efficacy of sequential double tracer subtraction and SPECT parathyroid imaging in the precise localization of a low mediastinal parathyroid adenoma successfully removed surgically. *Clin Nucl Med.*, 2004 Oct, 29(10)662-3. No abstract available. PMID: 15365449 [PubMed - indexed for MEDLINE]

RUBELLO D, CASARA D, GIANNINI S, PIOTTO A, DALLE CARBONARE L, PAGETTA C, BONI G, MARIANI G, MUZZIO PC, PELIZZO MR. Minimally invasive radioguided parathyroidectomy: an attractive therapeutic option for elderly patients with primary hyperparathyroidism. *Nucl Med Commun.* 2004 Sep, 25(9)901-8. PMID: 15319595 [PubMed - indexed for MEDLINE]

## PUBLICATIONS OF THE SCINTIRAD COLLABORATION

### Journal's articles

R. PANI, R. PELLEGRINI, M.N. CINTI, P. BENNATI, M. BETTI, F. VITTORINI, M. MATTIOLI, G. TROTTA, V. ORSOLINI CENCELLI, R. SCAFÈ, L. MONTANI, F. NAVARRIA, D. BOLLINI, G. BALDAZZI, G. MOSCHINI, P. ROSSI, F. DE NOTARISTEFANI, "LaBr<sub>3</sub>:Ce crystal: The latest advance for scintillation cameras", *Nuclear Inst. and Methods in Physics Research A*, 572(1) (2007) 268-269.

A. ANTOCCIA, G. BALDAZZI, A. BANZATO, M. BELLO, P. BOCCACCIO, D. BOLLINI, F. DE NOTARISTEFANI, U. MAZZI, L.M. ALAFORT, G. MOSCHINI, F.L. NAVARRIA, R. PANI, A. PERROTTA, A. ROSATO, C. TANZARELLA, N.M. UZUNOV, A YAP camera for the biodistribution of <sup>188</sup>Re conjugated with Hyaluronic-Acid in "in vivo" systems, *Nuclear Instruments and Methods in Physics Research A*, 571 (2007) 484-487

A. ANTOCCIA, A. BANZATO, M. BELLO, D. BOLLINI, F. DE NOTARISTEFANI, C. GIRON, U. MAZZI, L. MELENDEZ-ALAFORT, G. MOSCHINI, A. NADALI, F. NAVARRIA, A. PERROTTA, A. ROSATO, C. TANZARELLA, N.M. UZUNOV, <sup>188</sup>Rhenium-induced cell death and apoptosis in a panel of tumor cell lines, *Nuclear Instruments and Methods in Physics Research A* 571 (2007) 471-474

V. ORSOLINI CENCELLI, F. DE NOTARISTEFANI, E. D'ABRAMO, High Speed Readout for the H8500 Flat Panel PSPMT, *Nuclear Instruments and Methods in Physics Research A*, 571 (2007) 389-391

R. SCAFÈ, R. PANI, R. PELLEGRINI, G. IURLARO, L. MONTANI, MARIA NERINA CINTI, Si-APD readout for LaBr<sub>3</sub>:Ce scintillator, *Nuclear Instruments and Methods in Physics Research A*, 571 (2007) 355-357

PANI, R., PELLEGRINI, R.; CINTI, M.N., BENNATI, P., BETTI, M., VITTORINI, F.; MATTIOLI, M., TROTTA, G., ORSOLINI CENCELLI, V., R. SCAFÈ, F. NAVARRIA, D.

BOLLINI, G. BALDAZZI, G. MOSCHINI, F. DE NOTARISTEFANI, Ce doped lanthanum tri-bromide SPET scanner for molecular imaging, *Nuclear Instruments and Methods in Physics Research A*, 571(1-2) (2007) 187-190.

R. PANI, R. PELLEGRINI, M. BETTI, G. DE VINCENTIS, M.N. CINTI, P. BENNATI, F. VITTORINI, V. ORSOLINI CENCELLI, F. NAVARRIA, D. BOLLINI, G. MOSCHINI, G. IURLARO, L. MONTANI, F. DE NOTARISTEFANI, Clinical evaluation of pixellated NaI:Tl and continuous LaBr<sub>3</sub>:Ce, compact scintillation cameras for breast tumors imaging, *Nuclear Instruments and Methods in Physics Research A*, 571(1-2) (February 1, 2007) pp. 475-479.

C. D'AMBROSIO, F. De NOTARISTEFANI, G. HULL, V. ORSOLINI CENCELLI, R. PANI, Study of LaCl<sub>3</sub>:Ce light yield with a hybrid photomultiplier tube, *Nuclear Instruments and Methods in Physics Research A*, 567(1) (2006) 187-191.

F. CUSANNO, E. CISBANI, S. COLILLI, R. FRATONI, F. GARIBALDI, F. GIULIANI, M. GRICIA, S. LO MEO, M. LUCENTINI, M.L. MAGLIOZZI, F. SANTAVENERE, R.C. LANZA, S. MAJEWSKI, M.N. CINTI, R. PANI, R. PELLEGRINI, V. ORSINI CANCELLI, F. DE NOTARISTEFANI, D. BOLLINI, F. NAVARRIA, G. MOSCHINI, High-resolution, high sensitivity detectors for molecular imaging with radionuclides: The coded aperture option, *Nuclear Instruments and Methods in Physics Research A*, 569(2) (2006) 193-196.

R. PANI, R. PELLEGRINI, M.N. CINTI, P. BENNATI, M. BETTI, V. CASALI, O. SCHILLACI, M. MATTIOLI, V. ORSOLINI CENCELLI, F. NAVARRIA, D. BOLLINI, G. MOSCHINI, F. GARIBALDI, F. CUSANNO, G. IURLARO, L. MONTANI, R. SCAFÈ, F. DE NOTARISTEFANI, Recent advances and future perspectives of gamma imagers for scintimammography, *Nuclear Instruments and Methods in Physics Research A*, 569(2) (2006) 296-300.

R. PANI, P. BENNATI, M. BETTI, M.N. CINTI, R. PELLEGRINI, M. MATTIOLI, V. ORSOLINI CENCELLI, F. NAVARRIA, D. BOLLINI, G. MOSCHINI, F. GARIBALDI, F. DE NOTARISTEFANI, Lanthanum scintillation crystals for gamma ray imaging, *Nuclear Instruments and Methods in Physics Research A*, 567(1) (2006) 294-297.



ANTOCCIA A., BALDAZZI G., BELLO M., BERNARDINI D., BOCCACCIO P., BOLLINI D., DENOTARISTEFANI F., GARIBALDI F., HULL G., MAZZI U., MOSCHINI G., MUCIACCIO A., NAVARRIA F.L., ORSOLINI CENCELLI V., PANCALDI G., PANI R., PERROTTA A., RIONDATO M., ROSATO A., SGURA A., TANZARELLA C., UZNOV N., AND ZUFFA M., Preliminary study of metabolic radiotherapy with  $^{188}\text{Re}$  via small animal imaging, *Nuclear Instruments and Methods in Physics Research B* (Proc. Suppl.) 150 (2006) 411-416

F. GARIBALDI, R. ACCORSI, M. N. CINTI, E. CISBANI, S. COLILLI, F. CUSANNO, G. DE VINCENTIS, A. FORTUNA, R. FRATONI, B. GIROLAMI, F. GHIO, F. GIULIANI, M. GRICIA, R. LANZA, A. LOIZZO, S. LOIZZO, M. LUCENTINI, S. MAJEWSKI, F. SANTAVENERE, R. PANI, R. PELLEGRINI, A. SIGNORE, F. SCOPINARO, AND P. P. VENERONI, Small animal imaging by single photon emission using pinhole and coded aperture Collimation, *IEEE Trans. Nucl. Science* 52, Issue 3, Part 1 (2005) 573 - 579

N. UZUNOV, M. BELLO, P. BOCCACCIO, G. MOSCHINI, D. BOLLINI, F. DE NOTARISTEFANI, Measuring the imaged-object distance with a stationary high-spatial-resolution scintillation camera, *Physics in Medicine and Biology*, 51 (2006) N199-N204

LAURA MELÉNDEZ-ALAFORT, MATTIA RIONDATO, ANNA NADALI, ALESSANDRA BANZATO, DAVIDE CAMPORESE, PASQUALE BOCCACCIO, NIKOLAY UZUNOV, ANTONIO ROSATO, ULDERICO MAZZI, Bioavailability of  $^{99\text{m}}\text{Tc}$ -HA-Paclitaxel complex [ $^{99\text{m}}\text{Tc}$ -ONCOFID-P] in mice using four different administration routes, *Journ. of Labelled Compounds and Radiopharmaceuticals* 49 (2006)

UZUNOV N., BELLO M., BOCCACCIO P., MOSCHINI G., BALDAZZI G., BOLLINI D., DE NOTARISTEFANI F., MAZZI U., RIONDATO M., Performance measurements of a high-spatial-resolution YAP camera, *Physics in Medicine and Biology*, vol. 50 (2005) pp. N11-N21 ISSN: 0031-9155.

SCAFE' R., PELLEGRINI R., SOLURI A., MONTANI L., TATI' A., CINTI M.N., CUSANNO F., TROTTA F., PANI R., GARIBALDI, F., A study of intrinsic crystal-pixel light-output spread for discrete scintigraphic imagers modeling, *IEEE Trans. Nucl. Science* 51 (3) (2004) 80-84.

PANI, R.; CINTI, M.N.; DE NOTARISTEFANI, F.; PELLEGRINI, R.; BENNATI, P.; BETTI, M.; TROTTA, G.; KARIMIAN, A.; MATTIOLI, M.; GARIBALDI, F.; CUSANNO, F.; CENCELLI, O. Imaging performances of LaCl<sub>3</sub>:Ce scintillation crystals in SPECT, *Nuclear Science, IEEE Transactions on*, in press.

### Contributions to books

BASSO S., MAZZI U., BELLO M., DENOTARISTEFANI F., MOSCHINI G., ALOISI A., TUVE' C., POTENZA R. (2002). Administration of Tc-99m-Labelled Drugs by Cryoelectrophoresis. In NICOLINI M., MAZZI U. *Technetium, Rhenium and Other Metals in Chemistry and Nuclear Medicine*. (vol. 6, pp. 647-650). ISBN: 88-86281-73-0. PADUA: SGEditoriali (ITALY).

GIRON M.C., BELLO M., CALICETI P., MAZZI U., MOSCHINI G., ROSSIN R., VISENTIN R., BOLLINI D., DENOTARISTEFANI F., NICOLINI M. (2002). YAP-Camera device for biodistribution studies in mice of 99mTc-radiotracers. In NICOLINI M., MAZZI U. *Technetium, Rhenium and other Metals in Chemistry and Nuclear Medicine*. (vol. 6, pp. 555-557). PADUA: SGEDITORIALI.

ROSSIN R., ZORZET S., ZANELLA A., TURRIN C., SAVA G., MOSCHINI G., PERBELLINI A., MAZZI U. (2002). In vivo biodistribution studies on Hyaluronan Butyrate by means of 99mTc direct labelling and YAP camera. In NICOLINI M., MAZZI U. *Technetium, Rhenium and other Metals in Chemistry and Nuclear Medicine*. (vol. 6, pp. 689-693).

BELLO M., CALICETI P., MOSCHINI G., ET AL. (1998). Biodistribution studies in rats of on market Tc radiopharmaceuticals by means of a YAP-Camera. In NICOLINI M., MAZZI U. *Technetium, Rhenium and Other Metals in Chemistry and Nuclear Medicine*. (vol. 5, pp. 49 - 52). ISBN: 8-86281-35-8. XI National Congress on Research activities in Radiochemistry, Radiation Chemistry, Nuclear and Radioelements Chemistry, Rome 30/9-2/10, 1998. PADUA: SGEditoriali (ITALY).

## Proceedings

A. ANTOCCIA, G. BALDAZZI, M. BELLO, D. BERNARDINI, P. BOCCACCIO, D. BOLLINI, F. DE NOTARISTEFANI, U. MAZZI, G. MOSCHINI, A. MUCIACCIO, F. NAVARRIA, G. PANCALDI, A. PEROTTA, M. RIONDATO, A. ROSATO, A. SGURA, C. TANZARELLA, N. UZUNOV, M. ZUFFA, Preliminary study of metabolic radiotherapy with  $^{188}\text{Re}$  via small animal imaging, *Nucl. Phys. B (Proc Suppl.)* 150 (2006)

R. PANI R., CINTI M. N., PELLEGRINI R., DE NOTARISTEFANI F., BENNATI P., BETTI M., TROTTA G., MATTIOLI M., GARIBALDI F., ORSOLINI CENCELLI V., MOSCHINI G., AND NAVARRIA F., "LaBr<sub>3</sub>:Ce scintillation camera", *IEEE Nuclear Science Symposium Conference Record*, Volume 4, 23-29 Oct. 2005 Page(s):2061 - 2065

ANTOCCIA A., G. BALDAZZI, M. BELLO, P. BOCCACCIO, D. BOLLINI, F. DE NOTARISTEFANI U. MAZZI, MOSCHINI G., A. MUCIACCIO, F.-L. NAVARRIA G. PANCALDI, A. PERROTTA, M. RIONDATO, A. ROSATO, A. SGURA, C. TANZARELLA, M. ZUFFA. (2005). Study of metabolic radiotherapy with  $^{188}\text{Re}$  via small animal imaging. X Workshop on Nuclear Physics - *Wonp' 2005. Habana*, February 7-10, 2005.

ANTOCCIA A., G. BALDAZZI, M. BELLO, D. BERNARDINI, P. BOCCACCIO, D. BOLLINI, F. DE NOTARISTEFANI, U. MAZZI, MOSCHINI G., A. MUCIACCIO, F. L. NAVARRIA, G. PANCALDI, A. PERROTTA, M. RIONDATO, A. ROSATO, A. SGURA, C. TANZARELLA, N. UZUNOV, M. ZUFFA. (2004). Study of metabolic radiotherapy with  $^{188}\text{Re}$  via small animal imaging. *9th Topical Seminar on Innovative Particle and Radiation Detectors*. 23 - 26 May 2004 Siena, Italy.

ANTOCCIA A., G. BALDAZZI, A. BANZATO, M. BELLO, D. BOLLINI, D. CAMPORESE, F. DE NOTARISTEFANI, U. MAZZI, MOSCHINI G., F. NAVARRIA, M., A. PERROTTA, M. RIONDATO, A., ROSATO, A. SGURA, C. TANZARELLA. (2004). DATI PRELIMINARI SULLA BIODISTRIBUZIONE E DANNO AL DNA DEL  $^{188}\text{Re}$  IN SISTEMI "IN VITRO" ED "IN VIVO". *XII Convegno Nazionale SIRR*. 9 dicembre 2004.

ANTOCCIA A., A. BANZATO, M. BELLO, D. BOLLINI, D. CAMPORESE, F. DE NOTARISTEFANI, U. MAZZI, MOSCHINI G., F. NAVARRIA, M. RIONDATO, A. ROSATO, A. SGURA, C. TANZARELLA. (2003). DATI PRELIMINARI SULLA BIODISTRIBUZIONE E



N. UZUNOV, M. BELLO, P. BOCCACCIO, G. MOSCHINI, D. BOLLINI, G. BALDAZZI, F. DE NOTARISTEFANI, Accurate determination of the imaging properties of a high-spatial-resolution YAP camera, *LNL-INFN (REP)* 2004

N. M. UZUNOV, M. BELLO, P. BOCCACCIO, G. MOSCHINI, D. BOLLINI, A. PERROTTA, G. BALDAZZI, F. NAVARRIA, Spatial resolution of a position-sensitive imaging camera for small-animal imaging with  $^{188}\text{Re}$ , *LNL-INFN (REP)* 2005

A. ANTOCCIA, G. BALDAZZI, A. BANZATO, M. BELLO, D. BOLLINI, D. CAMPORESE, F. DE NOTARISTEFANI, C. GIRON, U. MAZZI, L. MENDEZ ALAFORT, G. MOSCHINI, A. NADALI, F. NAVARRIA, A. PERROTTA, M. RIONDATO, A. ROSATO, A. SGURA, C. TANZARELLA, N. M. UZUNOV, DNA damage and apoptosis induced by  $^{188}\text{Rhenium}$  in tumour cells, *LNL-INFN (REP)* 2005

Enquires about copyright and reproduction should be addressed to:

INFN - Laboratori Nazionali di Legnaro  
Annual Report Editors  
Viale dell'Università, 2  
35020 Legnaro (PD)  
Italia

Tel: (+39)0498068311  
Fax:- (+39)049641925

Requests for additional copies of the report should be addressed to:

Sig. Silvano Piva  
Biblioteca  
INFN - Laboratori Nazionali di Legnaro  
Viale dell'Università 2  
35020 Legnaro (PD)  
Italia

Tel: (+39)0498068397  
Fax: (+39)049641925

The Legnaro National Laboratories do not accept any responsibility for loss or damage arising from the use of information contained in any of their reports or in any communication about their tests or investigations.

